'OCEANS & LAKES'

INTERUNIVERSITY MASTER IN MARINE AND LACUSTRINE SCIENCE AND MANAGEMENT

Sedimentation in response to sea level rise in the mangroves of Mwache Creek, Mombasa-Kenya: a field and modeling study.

KIMELI Amon Kibiwot

August, 2013

Thesis submitted in partial fulfillment for master degree in Marine and Lacustrine Science and Management.

Promotor : Prof. Dr. Stijn Temmerman

Co-Promotor : Prof. Dr. Nico Koedam

Local Supervisor : Dr. Charles Magori

Local Supervisor : Dr. Jared Bosire

Table of Contents

List of Figures

List of Tables

Abstract

The stability of mangrove ecosystems in the face of rising sea level highly depends on their ability to maintain their surface elevations relative to the rising sea level through the accumulation of mineral and biotic sediments. To gain an understanding regarding the magnitude and interaction of sedimentation processes and other environmental factors with mangrove surface elevation, a study was carried out in Mwache Creek, Mombasa-Kenya, considered an appropriate site for this objective.

Suspended sediment concentrations (SSC), sediment accretion rates, soil vertical elevation change and variation of water levels were measured at two sites with varying degree of degradation due to human and natural impacts. Short term sediment accretion rates averaged between 51.78 – 144.48 g m^{-2} to 190.88 – 344.33 g m^{-2} in the highly degraded and the less degraded site respectively per 14-day spring-neap cycle. SSC varied on average between 0.076 g L^{-1} to 0.128 g L^{-1} in highly degraded site and the less degraded site respectively, while the average elevation change rates (mm yr^{-1}) varied between 1.65 mm yr^{-1} to 3.95 mm yr^{-1} in the highly degraded and the less degraded site respectively. The sea level in Mombasa was found to be rising at a rate of 3.1 mm yr^{-1} and this correlated well with IPCC projected global rates of 3.0 mm yr^{-1}. Using the data collected as part of this project, we applied a marsh sedimentation (MARSED) model to forecast the response of mangrove surface elevation to the effects of different environmental conditions by varying the model input variables. The model simulations showed that the growth of mangrove surface elevation is influenced by its elevation relative to sea level (which controls inundation and hence sediment supply by the tides), suspended sediment concentrations, mineral sediment accretion and compaction rates but the effect of organic sedimentation and low settling velocities were found to have a minimal effect.

From the observed accretion rates and elevation changes the mangroves of Mwache Creek act as sediment traps which is in agreement with previous research in both temperate and tropical coastal wetlands. However in Kenya, more short-term measurements and quantification of these sedimentation processes would provide further understanding of the integrity and sustainability of mangrove ecosystems in the face of global threats including relative sea level rise.

Keywords: Mwache Creek; mangroves; suspended sediment concentration; accretion; elevation change; sea level rise; modeling.

1. Introduction

Mangrove forests in Kenya are spread across the entire coastline and clustered mainly in deltas, creeks, protected bays and estuaries (Kairo *et al*., 2002; Kirui *et al*., 2006; Mohamed *et al*., 2009). Mangroves provide goods and services that are of ecological, economic and environmental importance (Krauss *et al*., 2010) and their global coverage has gradually declined to an estimated areal coverage of 152,000 km^2 (Spalding *et al*., 2010). The Kenyan coast is estimated to be covered by approximately 450 km^2 of mangroves by the year 2010, and 18 % was lost between 1985 and 2010 mainly due to human extraction for fuel, timber and clearance for alternative land uses including aquaculture and salt works (Kirui *et al*., 2012).

Mangroves are threatened by natural coastal hazards including flooding and sea level rise (accelerated by climate change) and anthropogenic impacts. Tsunamis which are geological in nature (Alongi, 2008) and based on their unpredictability, magnitude and often catastrophic effects (Cochard, *et al*., 2008) are also a major threat to mangrove ecosystems. While sea level rise is a major threat for mangrove ecosystems in the long-term (Gilman *et al*., 2008; Saad *et al*., 1999), immediate indirect threats such as floods, tsunamis and large sudden sedimentation events (Bosire *et al*., 2006; Kitheka *et al*., 2003), pose a reasonable challenge compromising the integrity of mangrove forests and dependent livelihoods. Relative sea level rise is a major threat to mangrove ecosystems since it is believed to contribute to the recent and projected future loss of coastal wetlands through inundation of existing coastal mud flats, tidal marshes and mangroves forests (Gilman *et al*., 2008). Climate change will lead to accelerating sea level rise and therefore mangroves will face the stresses and threats brought about by this phenomenon (Alongi, 2008). However, mangroves can respond and subsequently adapt to sea-level rise if it occurs slowly enough (Ellison & Stoddart, 1991), and if enough space for expansion exist.

Sediment accretion and surface elevation changes (which includes subsurface processes) in response to sea level rise have been studied intensively in tidal salt marshes, and relatively less in mangrove ecosystems. Mangrove forests can be considered as the tropical equivalent of tidal salt marshes because they occupy the same intertidal locations along the coast and are very complex ecological ecosystems affected by several physical factors including sea level rise and sedimentation (Alongi, 2008; Bosire *et al*., 2006;

Furukawa *et al*., 1997; Gilman *et al*., 2008; Kirwan & Temmerman, 2009; McKee, 2011). As a result sedimentation studies often referred to in this study have been carried out in tidal salt marshes. However, the few studies done in tropical mangrove ecosystems show that rates of mineral sediment accretion and subsurface accumulation of mangrove roots have assisted mangroves in adjusting to rising sea level (Cahoon & Lynch, 1997; McKee & Faulkner, 2000a; McKee *et al*., 2007). Mineral and organic sediment accretions due to terrigenous and tidal input have also been reported to control surface elevation in mangrove ecosystems (Cahoon & Lynch, 1997; McKee, 2011; Kumara *et al*., 2010; Woodroffe, 1992, 1985). Mangrove root structures which are species specific also control the rates of sediment accretion. It has been reported that intensity of sediment accretion is largest for trees with complex root matrix such as *Rhizophora* sp. and smallest for trees with simple surface knee roots such as *Ceriops* sp. (Furukawa & Wolanski, 1996; McKee, 2011; Tomlinson, 1986).

The integrity of the existing marsh and mangrove ecosystems is highly dependent on the ability of the system to keep pace with the rising sea level by maintaining its surface elevation relative to sea level (Cahoon *et al*., 1995; McKee *et al*., 2007; Saad *et al*., 1999). This ability is a function of mineral and organic sediment accretion (Fig. 1) (Alongi, 2008; Cahoon *et al*., 1995; McKee *et al*., 2007; French, 2006; Furukawa *et al*., 1997; Temmerman *et al*., 2003a, 2004) and therefore an understanding of the interaction between the mangrove ecosystem and these processes will assist in assessing and predicting the response of mangroves to rising sea level. Spatial variation in sediment accretion rates and elevation changes in the mangrove forests of Kenya is less studied and a clear understanding of the interaction between the mangrove ecosystem, sediment accretion and the rates of elevation change coupled with tidal influence is vital. Previously, studies on sea level, tidal current velocities, and sediments in Mwache Creek have been carried out to determine the dynamics of sediment exchange between the creek main channel and the mangrove forests (Kitheka *et al*., 2002, 2003).

Studies have shown that mangrove and marsh elevation is a function of surface elevation change (Allen, 1990; Cahoon *et al*., 1995; French *et al*., 2006; Kumara *et al*., 2010; Temmerman *et al*., 2004) due to accretion of mineral and organic sediments (brought by rivers and tides accelerated by sea level rise) and sediment compaction (Fig. 1). The friction caused by dense mangrove vegetation slows tidal currents, and reduced velocity and

increased duration of inundation is conducive for accretion of sediment particles in suspension (Alongi, 2008; French, 2006; McKee *et al*., 2007).

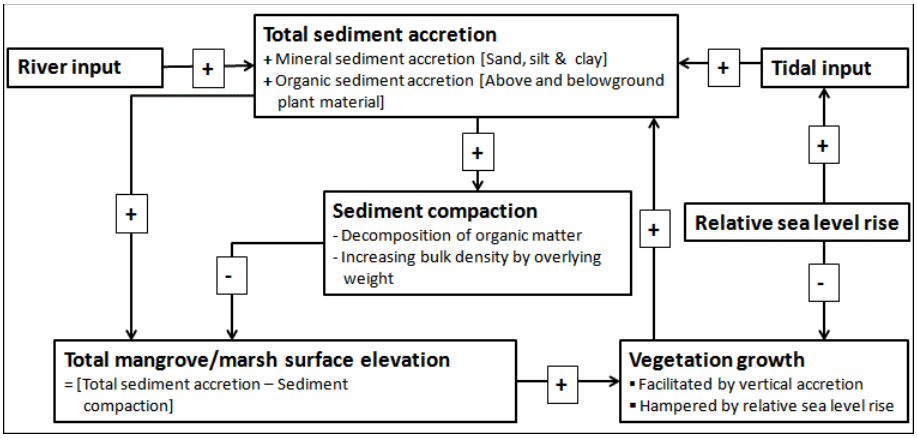

Figure 1: Conceptual model of the simplified interactions that control marsh/mangrove elevation (modified from Fagherazzi *et al*., 2012; French, 2006; Rybcyzk *et al*., 1998). Assumption is that erosion in vegetated tidal marsh/mangrove forest is negligible. In the text, total sediment accretion is also referred to as total sediment deposition and/or sedimentation.

Over the last two decades, several models (Allen, 1990, 1995, 1997; D'Alpaos *et al*., 2007a; French, 2006; Rinaldo *et al*., 1999a; Rybczyk *et al*., 1998; Temmerman *et al*., 2003a, 2004, 2005b; Wang, 2010) have been developed in order to simulate the response of tidal marsh surfaces to sea level rise. However, these salt marsh models have a limited realm of effectiveness due to their different spatial scales under consideration, the processes to be simulated and the final model outputs (Fagherazzi *et al*., 2012).

Zero-dimensional point models (including Allen, 1990; French, 2006; Temmerman *et al*, 2003a, 2004) simulate processes including vertical marsh growth due to sediment accretion with time at a single point being considered representative for the whole marsh/mangrove platform. However, these models do not incorporate the feedback mechanisms between physical processes (including erosion) and vegetation (Fagherazzi *et al*., 2012). Excluding these important processes, the model misses vital interactions within the whole system that ideally influences net marsh/mangrove surface growth and reduces the confidence of the model outputs. However, French, (2006) incorporated the effect of auto-compaction of early sediment accretions negating the idea that sediment accretion directly translates into elevation changes. Auto-compaction causes thinning as initial sediment accretions are dewatered and compressed due to overlying weight. Temmerman *et al*. (2003a, 2004) incorporated suspended sediment concentrations as a function of time

as tidal height increase with incoming tides.

Two-dimensional and one-dimensional models are spatially more representative than the zero-dimensional models because they account for spatial variations of processes in their simulations (Fagherazzi *et al*., 2012). These models simulate morphodynamics across a marsh platform (two-dimensional) or marsh transects (one-dimensional) and incorporate more processes including sediment accretion, channel development and erosion in their simulations. However, increasing the number of processes to be simulated increases the complexity of the models (Fagherazzi *et al*., 2012). The two-dimensional model of Rinaldo *et al*. (1999a) assumed a flat marsh platform (therefore excludes the effect of marsh/mangrove elevation on inundation and ultimately sediment accretion rates), constant friction both in space and time (excludes the effect of different flow velocities in settling out of sediments in suspension). The model of D'Alpaos *et al*. (2007a) simulated the transport of suspended sediments on a marsh platform assuming that tidal channels are the sources of sediments but Temmerman *et al*. (2005a) showed that sheet flow from marsh edges contribute to sediment accretion in marsh platforms. Fagherazzi *et al*. (2012) observed that the models of Rinaldo *et al*. (1999a) and D'Alpaos *et al*. (2007a) are best suited to initial stages of a flood tide when the water depths are still relatively low.

The 3D model of Temmerman *et al*. (2005b) took into account the interaction between vegetation and marsh platform sediment accretion specifically accounting for the influence of the vegetation canopy on velocity and friction contrary to Rinaldo *et al*. (1999a). Despite most salt marsh models assuming that below ground production have a minimal effect on the overall sedimentation process and subsequent marsh growth, the model of Rybczyk *et al*. (1998) showed that increased belowground production and high rates of organic sediment accretion could have a profound effect on marsh elevation.

Large scale models have also been developed to simulate processes that influence marsh/mangrove surface growth over an entire coastline or estuary. These large scale models are aimed at reducing the computation of physical processes (Fagherazzi *et al*., 2012) therefore simplify them and expand the spatial resolution of resultant effects. These models incorporate several environmental factors including subsidence, river discharge and climate variability and therefore are able to model historical trends including land loss. However since the models simulate processes over large areas, extrapolations of these processes may lead to loss of critical information which are site specific.

Existing modeling studies for mangrove sedimentation in response to sea level rise are very scarce, but other models including the organic model of Chen & Twilley, (1999) simulating the vertical distribution of organic matter as well as mineralization in mangrove sediments have been developed. This model incorporated biogeochemical processes unique to forested coastal wetlands including litter production and wood decomposition, however, the model does not account for compaction in soil formation and therefore overestimating vertical growth of mangrove surface.

In this study we focused on one zero-dimensional model, MARSED, which has been previously applied to sedimentation in tidal marshes in the temperate Scheldt estuary (Temmerman *et al*., 2003a, 2004). This model incorporated initial suspended sediments concentration, C (0), and showed that sediment accretion rate over a whole inundation cycle increases linearly with maximum tidal height if C (0) is assumed to be constant, but if *C* (0) is taken as a function of inundation height, the sediment accretion rate grows exponentially.

1.1 Objectives of the study

1.1.1 Overall objective

The overall objective is to apply and determine the effectiveness of an existing marsh sedimentation (MARSED) model used for sedimentation in tidal marshes (Scheldt estuary, Belgium) to sedimentation in tropical mangrove ecosystems (in this study Mwache Creek, Kenya) in order to explore the response and/or resilience of mangrove ecosystems to different scenarios of environmental conditions, such as different supply of suspended sediments and different rates of relative sea level rise. The specific objectives are:

1. To determine the variation of the suspended sediment concentrations, sediment accretion rates, short-term rates of elevation changes and water levels in Mwache Creek based on field measurements during a period of one year and during spring-neap tidal cycles.

2. To simulate model scenarios by varying the input variables, in order to identify the critical environmental conditions for which the mangroves in Mwache Creek are able to keep up with sea level rise or not.

2. Study approach and methodology

2.1 Description of study area

The field study was carried out in a shallow tidal Creek in Mwache, Mombasa – Kenya (Fig. 3) connected to the Indian Ocean through the Port-Reitz channel. The total area of the wetland is approximately 17 km^2 (Kitheka *et al*., 2002, 2003) with about 70 % of the surface area covered by the common mangrove species *Avicennia marina, Rhizophora mucronata, Ceriops tagal, Bruguiera gymnorrhiza* and *Sonneratia alba*. Mangrove zonation studies in Kenya (Bosire *et al*., 2003; Dahdouh-Guebas *et al*., 2002; Matthijs *et al*., 1999) have shown a common pattern of species variation with distance from the sea. *S. alba* with a mixture of few *R. mucronata* have been found to form narrow strips close to the sea followed by a mixed zone comprising of *R. mucronata*, *C. tagal* and *B. gymnorrhiza* species whereas further landwards in the high intertidal zone *A. marina* and *C. tagal* dominate.

Like other parts of the Kenyan coast, Mwache Creek is influenced by two monsoon seasons (Mohamed *et al*., 2008; Schmitz *et al*., 2006). The long rains between April and August are influenced by the south-east (SE) monsoon while the short rains between October and November are influenced by the north-east (NE) monsoon (Fig. 2). The creek is tidally – dominated and it experiences a semi-diurnal tidal regime with a tidal range of 3 - 1.4 m in the main channel, 0.9 – 2.5 m in the mangrove forest and 1.3 - 3 m during neap and spring tides respectively (Kitheka *et al*., 2002, 2003).

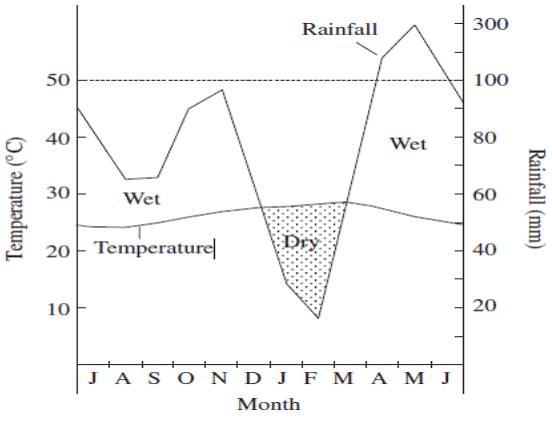

Figure 2: A general climate diagram of Mombasa-Kenya adapted from Schmitz *et al*. (2006); original source, Lieth *et al*. (1999)

Mwache Creek receives freshwater and terrigenous sediments from the seasonal Mwache River with highest discharge (up-to 40 $m^{-3}s^{-1}$) during the rainy season (Kitheka *et*

al., 2002). Due to heavy supply of terrigenous sediments during the El Niño of 1997–1998, approximately 10^6 tonnes of sediments were deposited in the wetland causing massive destruction of the mangrove forest in the Creek (Bosire *et al*., 2003; Kitheka *et al*., 2002). According to Kitheka *et al*., 2002, suspended sediment concentrations (SSC) and grain size along Mwache Creek reduces with increasing distance from the sea reflecting reduced tidal current velocities in the creek and therefore progressive sediment accretion in the creek with increasing distance from the sea.

Mwache Creek is characterized by two sections (Fig. 3) with varying levels of environmental degradation (see appendix A). One section is highly degraded partly due to

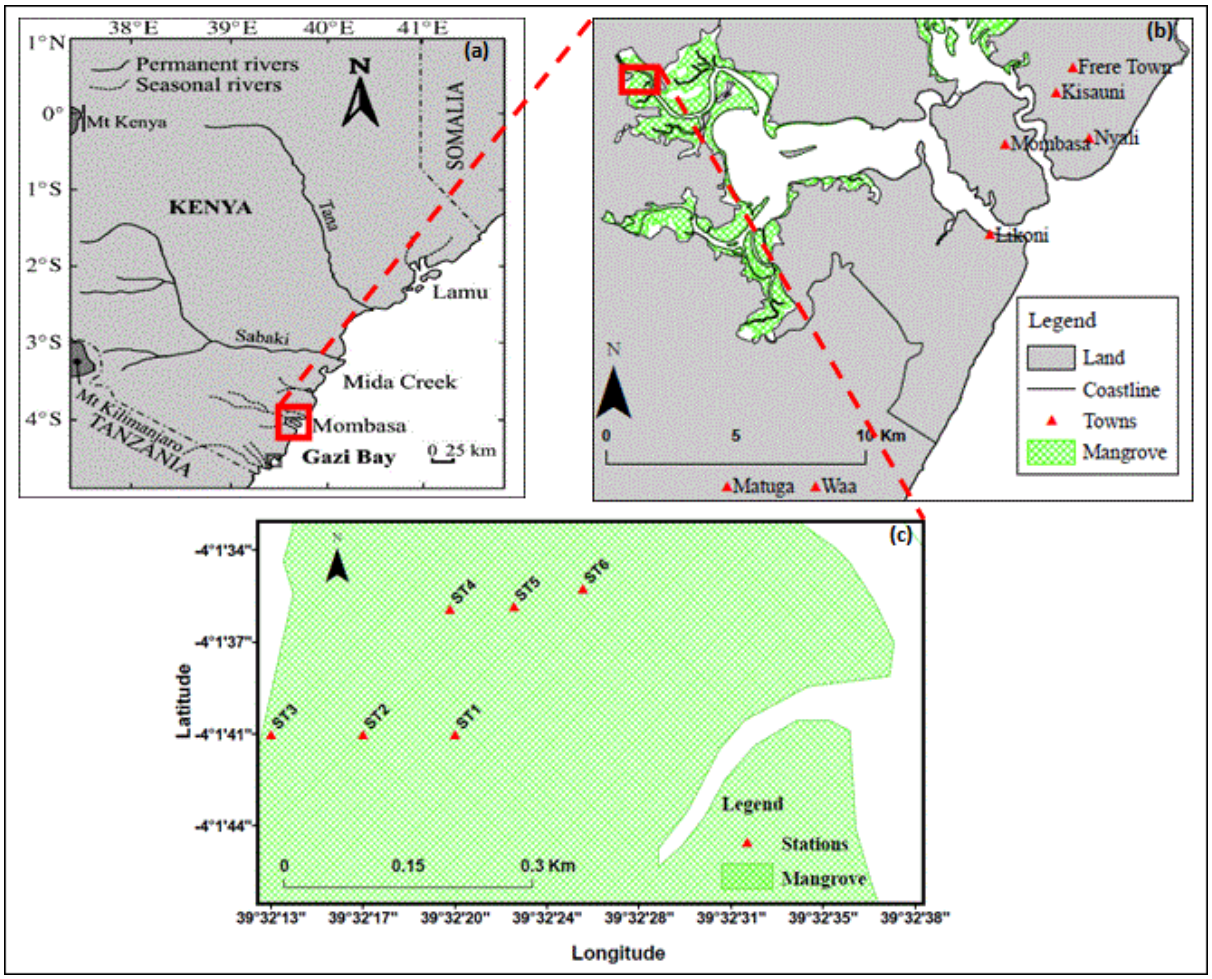

Figure 3: Map showing the study sites at Mwache (a) Kenya with its boundaries and coastline (Source: Modified from Bosire *et al*., 2003) (b) Mombasa and its environs (c) Study site at Mwache (Source: ArcMap generated, data obtained from Kenya Environmental, Sensitivity Atlas (KENSEA) project (2006)).

the effect of massive sedimentation during the 1997/1998 *El-Niño* rains and human exploitation. Another less degraded section is present, which is more pristine and less affected by either natural or human impacts.

Stations 1, 2 and 3 of our study were situated in the highly degraded section characterized by a similarly patchy vegetation cover of *A. marina* mixed with few *R. mucronata* and *C. tagal*, bare sandy sediments and dead wood stumps. These stations are also the farthest from the creek channel and this is supported by the presence of characteristic high intertidal mangrove species as discussed earlier. Cores taken from these sites show that there is a sandy top layer representing freshly deposited sediments but with increasing depth, dark anoxic clay layers including plant debris were discernible.

Stations 4, 5 and 6 of our study were situated in the less degraded section characterized by a dense mixed vegetation cover dominated by *R. mucronata* and *S. alba* and interspersed with *A. marina*. These stations are also closest to the creek channel and this correlates well with the characteristic zone of dominant mangrove species. Cores taken from these sites showed a characteristic fine-textured top layer of sediments, probably attributable to the thick mangroves reducing water velocity and aiding the settling of these very fine sediments. The top sediments are clayey silt and the bottom deep sediments exhibit the dark colored anoxic sediments with a few root debris.

2.2 Experimental details

2.2.1 The Model

The marsh sedimentation model (MARSED) (see Temmerman *et al*., 2003a, 2004) used in this study, is based on a zero-dimensional time stepping approach to simulate vertical marsh growth due to sediment accretion with time at one point on a marsh/mangrove surface. In this model, the rate of change in marsh surface elevation E (in m relative to lowest astronomical tide, L.A.T) is described as;

$$\frac{dE}{dt} = \frac{dS_{min}}{dt} + \frac{dS_{org}}{dt} - \frac{dP}{dt} \quad \text{.....(1)}$$

where dS_{min} / dt is the rate of mineral sediment accretion, dS_{org}/dt the rate of organic sediment accretion and dP/dt is the rate of compaction of the accreted sediment, after dewatering, under younger sediment load. Furthermore, the yearly rate of mineral sediment accretion is further specified as:

$$\frac{dS_{min}}{dt} = \int_{year} \int_{T} Ws\, C(t)\, dt / \rho \quad \text{.....(2)}$$

Equation 2 shows that mineral sediment accretion is modeled as a product of the settling velocity, W_s (m s^{-1}), the time varying suspended sediment concentration C (g L^{-1}) at every time step t during a tidal cycle and ρ representing the dry bulk density. Equation 2 is integrated over every tidal cycle with a duration T and over every year in the simulated period. The compaction rate dP/dt was simulated yearly (Equation 1) to exclude influence of compaction of fresh sediments (Allen, 1990; Cahoon *et al*., 2000; French 2006; Temmerman *et al*., 2003a), which is already included in the value for the dry bulk density, ρ (Equation 2), approximated at 590 kg m^{-3} based on field measurements (see further below). Using the average percentage soil organic matter (SOM) and average accretion rates measured in the field (see further below for the field measurements), the rate of organic sediment accretion (dS_{org}/dt) was determined by the equation below:

$$dS_{org}/dt = SOM\ (\%) * Accretion\ rate\ (m\ yr^{-1}) \quad \text{.....(3)}$$

where *SOM* (%) is the average percentage of soil organic matter and the accretion rate representing the average rate of surface elevation determined from the sedimentation-erosion tables (see further below).

C (in g L^{-1}) is the suspended sediment concentration in the water above the marsh/mangrove surface and varies with time during tidal inundation. Due to wave and current attenuation by mangrove vegetation and therefore low flow velocities above the mangrove surface, Equation 2 assumes that there is no sediment resuspension (Temmerman *et al*., 2003a). The following equation (4) is used in order to calculate the suspended sediment concentration $C\ (t)$ at any time step t during a tidal inundation:

$$d[h(t) - E]\ C(t) / dt = -W_s\ C(t) + C(0)\ dh / dt \quad \text{.....(4)}$$

where $h\ (t)$ is the time dependent water level, E (m L.A.T) is the marsh or mangrove surface elevation for a given year while C (0) is the incoming suspended sediment concentration in the water that floods the marsh or mangrove. Equation (4) describes the change in suspended sediment mass above a unit area of the marsh or mangrove surface (first term of equation (4)), as a result of the vertical settling of suspended sediment (second term) and lateral flux of water with a suspended sediment concentration $C\ (0)$ (third term). $C\ (0)$ has a specific value during the flood tide (when $dh/dt > 0$), while during the ebb tide (when dh/dt

< 0) *C (0)* is set to equal *C (t)*.

The tidal temporal variation of sea level, *h (t)*, within one spring-neap cycle is modeled based on the average tidal curve of Mombasa (Fig. 4a) derived from Mombasa tide gauge data. This average tidal curve fluctuates with the crest of the curve signifying periods of inundation. Sea level, *h (t)* can then be calculated for any tidal inundation with a high-water level $h\ (t_{HW})$ as:

$$h\ (t) = a * 1/(1 + (t\text{-}x_o / b)^2 + h\ (t_{HW}) - h\ (t_{mHW})) \quad \text{.....(5)}$$

where ***a***, ***b*** and x_0 are constants (***a***= maximum asymptote ; ***b*** = slope ; x_0 = Inflection point of curve) and $h\ (t_{mHW})$ = the mean high-water level (m L.A.T.) at Mombasa.

Equations 5, 4 and 2, enable the mineral sediment accretion rate, *dSmin/dt*, to be calculated for every single tidal inundation with a certain high-water level *h (tHW)*. The annual mineral sediment accretion rate, *dSmin/dt*, can now be calculated from the frequency distribution of high-water levels simulated for every year. This was done by considering the annual succession of mean high-water level (mHWL) at Mombasa and the yearly-averaged frequency distribution of high-water levels (Fig. 4b) around mean sea level at Mombasa, which is the nearest tide-gauge station. This was done by determining the daily mean high water levels (m L.A.T) representing the two maximum water levels of the semi diurnal tide and the frequency distribution determined relative to the mean sea level of Mombasa as recorded by the tide gauge.

The exceedance probability is defined as the chance (%) that a given high water level will be equaled or exceeded. The exceedance probability, P is modeled as;

$$P\ (HWL_{rel} > X) = a * exp\ (b*(1\text{-}exp(c*X))) \quad \text{..... (6)}$$

Where HWL_{rel} is the mean high water level relative to the average sea level and ***a***, ***b*** **and** ***c*** are constants derived by fitting a modified negative gompertz curve model on the observed curve (Fig. 4b) (here ***a*** = 102.5107, ***b*** = 0.1277 and ***c*** = 1.668 and *P* = Exceedance probability (%).

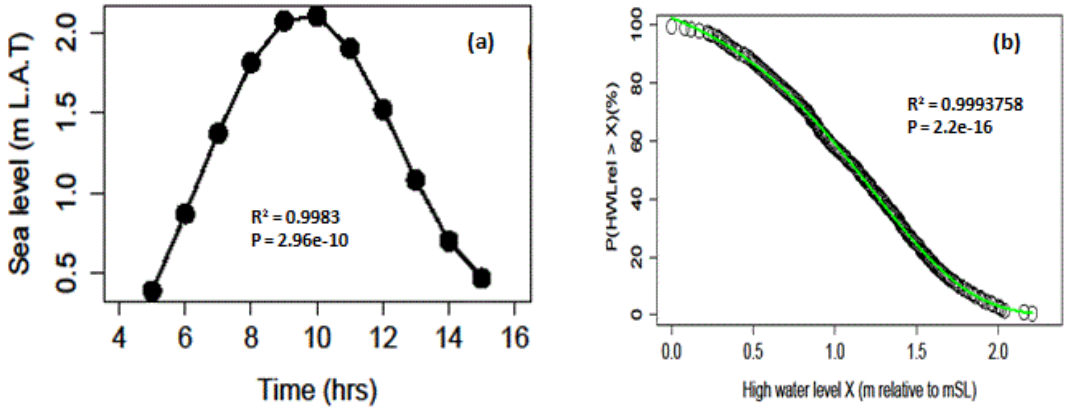

Figure 4: (a) Observed averaged tidal curve of Mombasa for the whole year (2012) fitted with a 6th order polynomial. (b) Frequency distribution curve showing the exceedance probability, P (%) of high water level (HWL) relative to the mean sea level at Mombasa fitted with a negative gompertz model curve.

The above described model is programmed in MATLAB and solves equation 5, 4 and 2 in pre-defined time steps of 300 s and equation 1 in time steps of 1 year (Temmerman *et al*., 2003a, 2004).

2.2.2 Data collection

A number of data were collected in the field in order to provide an estimate of the realistic range of input parameter values that needed to be used in the model. These data were collected within a two month period between July 20 and September 5, 2012; however Sedimentation-Erosion table data comprises of data from a year long (April 10, 2012 – April 26, 2013) monitoring program.

2.2.2.1 Suspended sediment Concentration (SSC): Using siphon samplers

Suspended sediment concentration (SSC) is expressed in grams of dry sediment per liter of water-sediment mixture (Wang, 2010). The concentration of suspended sediments (g L^{-1}) per spring-neap cycle was obtained from water samples that were collected using siphon samplers. Siphon samplers are water collecting bottles fitted with an intake and exhaust siphon tubes (See appendix B & D). The bottles are simply filled with water as soon as the tidal water level rises higher than the height of the siphon tube (Diehl, 2008).The siphon samplers were located in the path of incoming tides and this offered a reliable way to collect samples automatically from incoming tide (Furukawa *et al*., 1997). After every 14 days (after a full spring-neap cycle), the filled bottles were replaced. . In this way, only one water sample was taken instantaneously at one specific moment at the beginning of the

first flooding tide during the spring-neap tidal cycle.

The effectiveness of siphon samplers is minimized by variation in flow velocities causing irregular sampling (Diehl, 2008) and is vulnerable to damage from plant debris brought by incoming tides. Siphon samplers are also limited in ascertaining the exact time at which sampling begins (Edwards & Glysson, 1999) and this could lead to uncertainties. Two spring-neap cycles were sampled between July 20 and September 5, 2012 but suspended sediment concentration has been reported to be affected by seasonality (Wang, 2010) and variation in current speed. Therefore, the obtained SSC data for 2 spring-neap cycles must be considered as only indicative for the SSC values that can occur in the system, but do not allow to document temporal variations in SSC. Suspended matter was determined gravimetrically after filtration on dried Whatman GF/C filters and drying at 105 ^{o}C for 2 hrs to remove moisture (Maris *et al*., 2007; Temmerman *et al*., 2004).

2.2.2.2 Sediment accretion rates: Using sediment traps

During the same two month period, six sediment traps (diameter 0.20 m) were deployed and attached to the mangrove surface by pins and containing a filter paper on which sediments were deposited during tidal inundations of the mangrove surface (see appendix B). The filters were collected and replaced by clean ones after every 14 days taking into consideration the spring-neap tidal cycle (Temmerman *et al*., 2003b; Struyf *et al*., 2005). Samples that settled from suspension were removed from traps and rinsed with de-ionized water to remove salts and sieved to remove organic material. The sediments were then oven-dried at 105 ^{0}C for 8-12 hrs, and weighed to determine the accretion rate of suspended sediments (in g m^{-2} per spring-neap tidal cycle).

In turbulent waters, this method may be restricted to identification of only rapidly sinking particles (large particles) and therefore the fine sediments may be difficult to sample. However water flow velocities and turbulence are typically strongly reduced in tidal marsh vegetation (Leonard & Luther, 1995) and this may also be expected in mangrove vegetation. It is also difficult to ascertain the effects of resuspensions using this method, but due to the effect of marsh/mangrove vegetation on reduced flow velocities and turbulence, there is typically no resuspensions of deposited sediments (Christiansen *et al*., 2000). Sediment traps provide spot measurements and measure only sediment accretion but not elevation changes, therefore do not account for any subsurface processes (Thomas

& Ridd, 2004). This method is however effective when used together with SETs and feldspar markers (see below).

2.2.2.3 Sediment grain size and settling velocity

Surface sediments were also sampled at each of the six sampling stations during low tide. These sediment samples were collected in order to determine the grain size distribution and subsequently to estimate the settling velocity of the sediment based on the median grain size. Collection was done by gently scraping the surface (1-2 mm) (Saad *et al*., 1999). The Malvern 2000 laser diffraction method (©Malvern) was used to determine the grain size frequency distribution based on the Wentworth, (1922) grain size scale of clastic sediments. Organic components in sediments were first removed by adding 20 % hydrogen peroxide (H_2O_2) and the settling velocities were calculated using stokes law represented by the equation below:

$$W_s = g\, d^2\, (\rho_p - \rho_f) / (18 * \mu) \quad \ldots\ldots (7)$$

Where, W_s = Settling velocity (m s^{-1}), g = Gravitational acceleration (m s^{-2}), ρ_p & ρ_f = Mass density (kg m^{-3}) of particle and fluid respectively and μ = Dynamic viscosity (Ns m^{-2}) of water at 25 ^{0}C.

This procedure of determining the settling velocity only provides an approximate estimate of the settling velocity. In the model, a range of input values for the settling velocity were used (see further below) in order to assess the sensitivity of the model to input values for the settling velocity. From previous studies, it is already known that the model output is not so sensitive to variations in input values for settling velocity (Temmerman *et al*., 2004).

2.2.2.4 Sea and water levels: Using tide gauge and Divers

Tidal water level function h (t), time series (yearly mean) and tidal frequency distribution of high water level (HWL) were obtained from the Mombasa tide gauge data (04^o 04’ 30” S, 039^o 39’ 21.60” E) operated by Kenya Marine & Fisheries Research Institute (KMFRI) in collaboration with the University of Hawaii within the global sea level observing system (GLOSS) network. In this study, tidal data were used because the rate of accretion of sediment from tidal waters is directly proportional to the tidal flooding frequency, depth

and duration (Furukawa & Wolanski, 1997). The tidal water level fluctuation is modeled on two time scales: firstly the temporal variation of water level h (t) during one semidiurnal cycle based on data from the nearest tide gauge, and secondly the frequency distribution of high water levels h (t_{HW}) for every year (Temmerman *et al*., 2004).

The water levels (m L.A.T) were measured using the Mini D1701 diver instruments (©Schlumberger) designed to measure the water column height by measuring the water pressure. The Cera-diver measures the atmospheric pressure when it is not submerged and immediately it is submerged it measures the water and atmospheric pressure. By subtracting the atmospheric pressure, which is recorded with a Baro-diver that is placed on a high location (see appendix C) that is not submergible, the hydrostatic pressure is obtained, which can be transformed into a water column height above the mangrove surface.

Cera-divers were installed at stations 2, 4 and 5 and a Baro-diver installed at station 5 (see appendix C). The readings from the Baro-diver were used as representative of the whole study area since atmospheric pressure does not vary over short distances. The Cera-divers were tied to mangrove roots close to the surface (approx. 1 cm) to minimize the error when the divers were not submerged while the Baro-diver was tied as high as possible to avoid contact with water. The Cera-divers, however, do not take into account the effect of turbulent waves which could cause significant variation in the level of water above marsh/mangrove surface. Therefore, underestimating or overestimating the water depth (m) but this is possible only in regions affected by strong winds. Furthermore, waves are typically attenuated in dense vegetations (Moeller *et al*., 1996).

The difference of water pressure and atmospheric pressure gave the water depth (in m) above the mangrove sediment surface. The high water levels (HWL, m L.A.T) measured by the tide gauge were correlated with the calculated water depths at the mangrove sites at high tides. Since the system is characterized by a semidiurnal tide regime, the time when the two daily HWL (m L.A.T) were recorded in the tide gauge were correlated with the corresponding high water depth by the divers. This is because it is only during high water levels when highest pressure is recorded and therefore maximum water depth is obtained. The average of the difference between the corresponding tide gauge measurement (m L.A.T) and the water depth (m) measurement from the diver gave an approximate mangrove surface elevation (m L.A.T).

2.2.2.5 Sediment coring

Sediment cores were taken using 4.3 cm diameter PVC sediment corers (Bird *et al*., 2004). From the cores, 1 cm slices were sub-sampled every 10 cm for loss of ignition, grain size and dry bulk density analysis. This method has some limitations in that as the corer is pushed into the surface, compaction of sediments or pushing aside of sediments may occur reducing the actual depth of the samples sediment core, and also in loose non-cohesive sediments as the corer is raised after the coring there is a possibility of sediment loss (Callaway *et al*., 2012). This method is also cumbersome in highly vegetated mangrove ecosystems because the root structure of mangroves makes it almost impossible to core.

Sediment bulk density (g cm^{-3}) was measured using the dry weight of the sediment from each 10-cm sub-samples and was determined by 48 hrs of drying at 105 ^{0}C. Organic mineral content of each section was determined using the loss on ignition (LOI) method by burning a sediment sample in a muffle furnace at 450 ^{0}C for 8 hours according to a standardized method (EPA, 1983). Fresh sediments were oxidized with H_2O_2 before grain size analysis, which was done using the Malvern 2000 laser diffraction technique (©Malvern). Sediment compaction was deduced from dry bulk density of surface sediments and depth profiles (McKee *et al*., 2007; Temmerman *et al*, 2004; Vandenbruwaene *et al*., 2011). For this study, the compaction rate was deduced using the equation below (Bird *et al*., 2004; Temmerman *et al*., 2004).

$$dP / dt = P (\rho_o / \rho - 1) / dt \quad \text{.....(8)}$$

where dP/dt is the compaction rate in m yr^{-1}, P is thickness of sediment layer (m), ρ_o and ρ are the dry bulk densities (g m^{-3}) at the surface and at depth respectively.

2.2.2.6 Surface elevation and sediment accretion: Sedimentation-Erosion Tables (SETs) and Feldspar markers

The methodology used in this study entailed measuring the vertical sediment change (thickness) and dividing it by the duration of accretion (Cahoon & Lynch, 1997; McKee, 2011; Saad *et al*., 1999). In this study six sampling stations were each installed with a Sedimentation-Erosion Table (SET) and feldspar marker and field measurements taken every month for a whole year (April 2012 – April 2013). SETs were used to measure elevation change (including subsurface processes) and were placed adjacent to feldspar markers

spread on the soil surface and accretion above marker horizons indicated vertical accretion only (Boumans & Day Jr., 1993; Cahoon & Lynch, 1997). SETs are leveling devices attached to fixed datums (benchmark), normally steel rods driven to the surface as far as possible until refusal (Cahoon *et al*., 1995) to provide stable surfaces (see appendix B). The leveled table provided a stable reference for repetitive measurements recorded (in mm) relative to the fixed arm of SET. The SETs were set in 1 × 1 m plot in each site, measurements done monthly and a total of 12 replicates per monthly measurement (Cahoon & Lynch, 1997; McKee, 2011; Krauss *et al*., 2010) were averaged to get the monthly elevation change.

Accuracy of SET readings being an issue (McKee *et al*., 2007), one person was mandated to do the elevation change measurements for the whole monitoring period to minimize human errors. Measurements of SETs represents averaged surface elevations over the period between two observations (monthly in our study) and this restricts the potential of time variable measurements within the observation period (Cahoon *et al*., 2002; Thomas & Ridd, 2004). Accuracy of SETs measurements have been reported to be approximately ± 1.5 meters (Boumans & Day Jr., 1993; Thomas & Ridd, 1999) but this is based on numerous and continuous field measurements over time which lack in our Kenyan context and therefore interpretation of our field data could be inconclusive.

To obtain elevation change (in mm) over the twelve months (April, 2012 – April, 2013), the value of elevation in April 2012, was taken as the reference value and therefore fixed at a value of zero for all stations. All subsequent monthly measurements were then expressed as surface elevation change (mm) relative to the April, 2012 value. The annual rate of elevation change (in mm yr^{-1}) was obtained by getting the difference between April, 2013 and April, 2012 elevation values (in mm).

2.3 Data Analysis

Collected field data were analysed for the effect of vegetation disturbance on sedimentation variables in either the less or highly degraded site and for the influence of distance of stations from the main creek channel (the sediment source) on sedimentation variables. All statistical data analyses were done using the R software, Statistica V 8.0 and the Microsoft excel statistical package.

3. Results

3.1 Sediment budgets: Suspended sediment concentrations

There was a slight variation in suspended sediment concentrations (SSC) over the 14-day spring-neap tidal cycles (Fig. 5); furthermore, SSC variation showed a clear variation, 0.032 – 0.138 g L^{-1} in highly degraded to 0.067 – 0.203 g L^{-1} in the less degraded site per spring-neap cycle. High SSC values were also recorded in stations closest to the main creek channel.

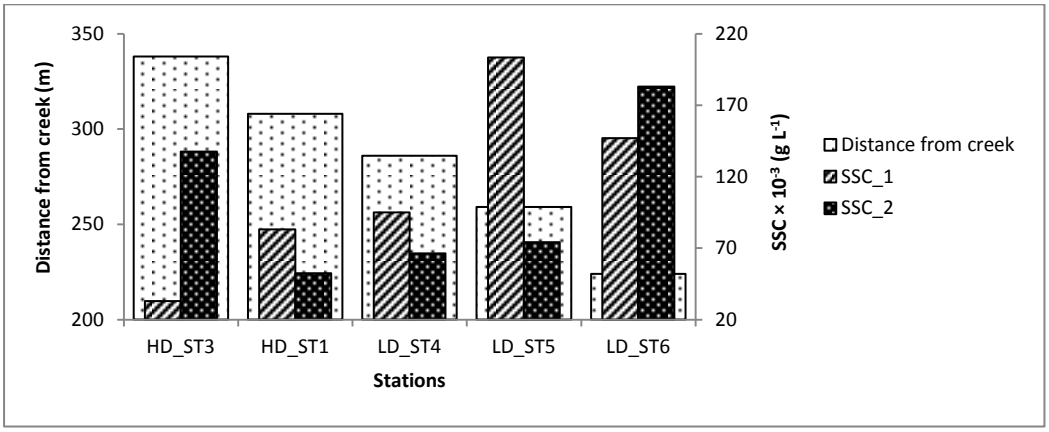

Figure 5: Variation of SSC with respect to sites (ST1 and ST3 both in highly degraded site & ST4-ST6 in less degraded site), spring-neap cycle (each 14 days) variation and relative distances of stations from the creek. HD = Highly degraded site and LD = Less degraded site.

The loss of ignition tests showed a relative variation of soil organic matter (SOM) between and within the two types of sites (Fig. 6) with the high SOM recorded in the less degraded sites and in the stations closest to the main creek channel (source of sediments). Dry bulk density showed a near-linear increase with depth (Fig. 7) and the regression analysis showed that the increase in dry bulk density is significant with increasing depth ($p = 0.012$).

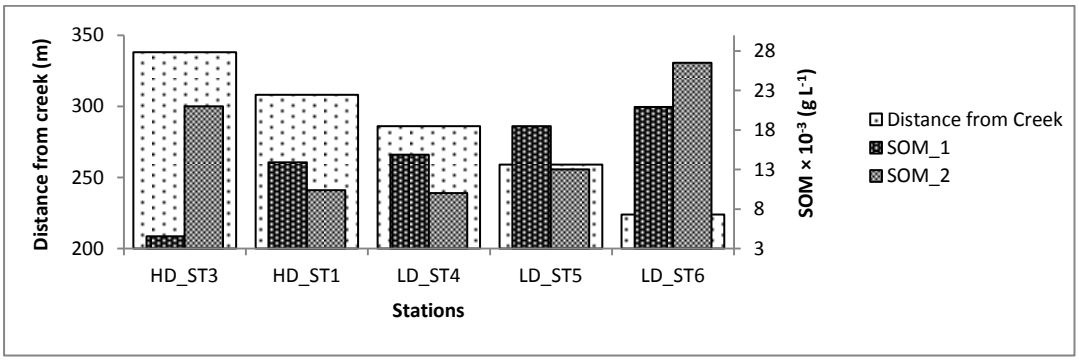

Figure 6: Variation of SOM with respect to sites (ST1 and ST3 both in highly degraded site & ST4-ST6 in less degraded site), spring-neap cycle (each 14 days) variation and relative distances of stations from the creek. HD = Highly degraded site and LD = Less degraded site.

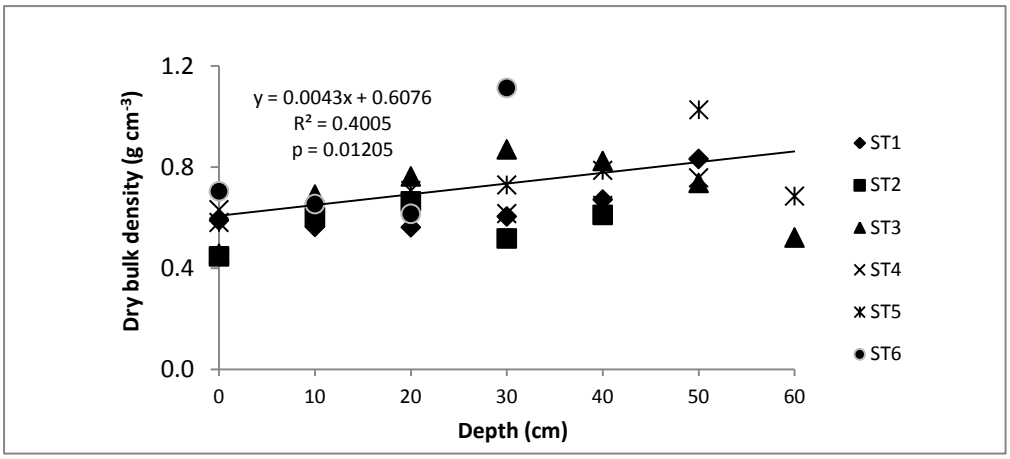

Figure 7: The near-linear relationship of variation in dry bulk density (g cm^{-3}) with depth from different stations with the regression line representing ST1.

3.2 Grain size analysis

Our study showed varying grain size distribution with depth and sand as the main characteristic sediment type with relatively small percentages of clay. Also a clear decrease of percentage of sand with depth is evident in both the highly and less degraded sites (Fig. 8, 9). Sand (63 – 250 µm) was found to be predominant in the highly degraded site however, in the less degraded site the percentage of silt and clay increased markedly (Fig. 9, 10).

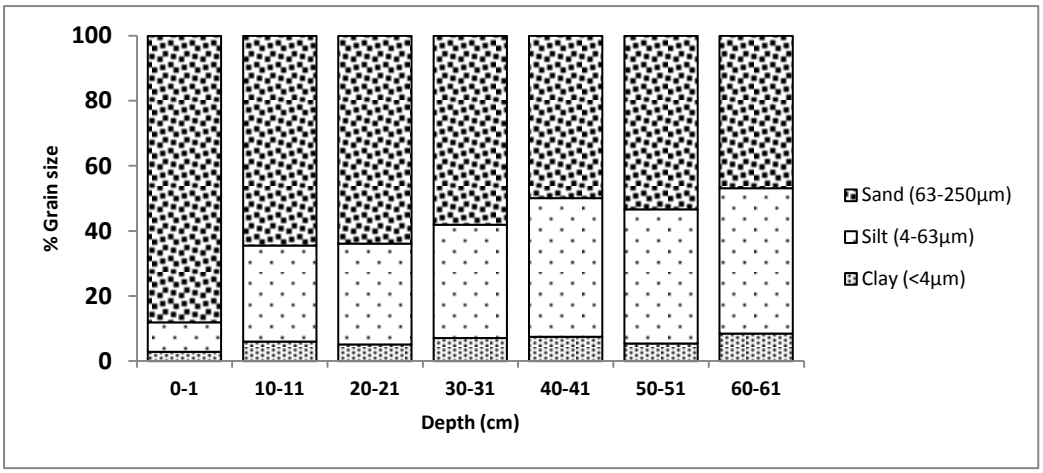

Figure 8: Grain size variation with depth in the highly degraded site with a clear evidence of decreasing percentage of sand with depth and an increasing percentage of silt and clay.

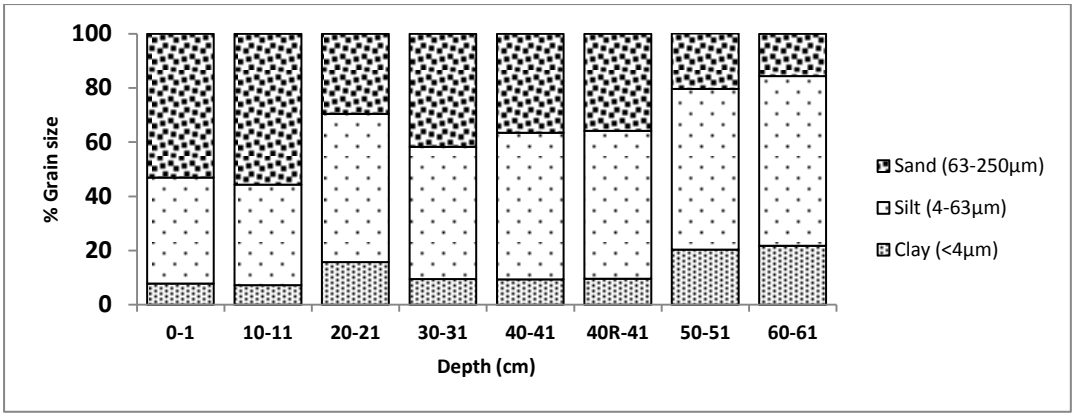

Figure 9: Grain size variation with depth in the less degraded site showing clear decrease of percentage of sand with depth and increasing dominance of silt and clay throughout the core profile.

Surface sediments also showed predominance towards a sandy sediment type with over 50 % of the sediment grain size being between 63 - 250 µm in both sites. A comparison of grain size distribution between stations showed that the highly degraded site (ST1,ST2,ST3) are characterized by predominantly sandy sediments, and the less degraded site (ST4,ST5,ST6) by relatively higher clay and silt contents (Fig. 10).

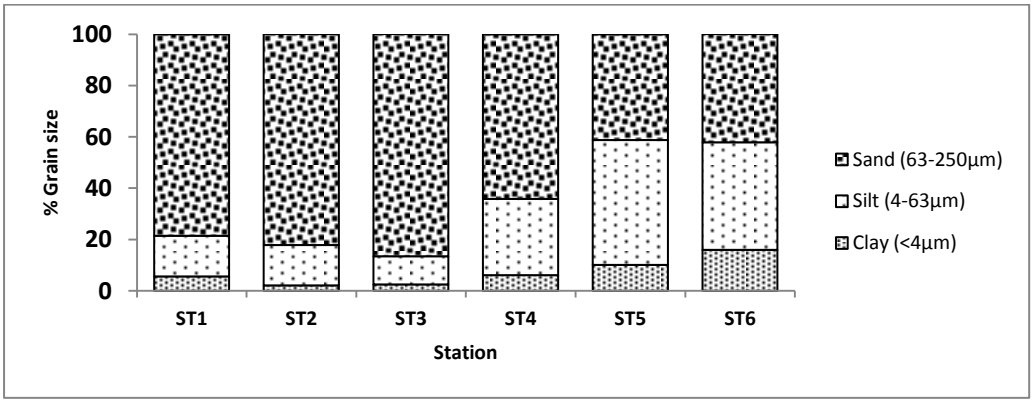

Figure 10: Grain size variation of surface sediments in highly (ST1, ST2 & ST3) and less degraded site (ST4, ST5 & ST6). Clay and silt increases in the less degraded part as compared to the highly degraded.

3.3 Sediment accretion rates: Feldspar markers and sediment traps

The accretions on the feldspar markers were too little to be measured, but with continued monitoring, measurable sediment accretion will occur. Accretion rates measured by sediment traps showed a spatial variation between the highly and less degraded site, with higher accretion in the less degraded site (Fig. 11), ranging from 190.88 – 344.33 g m^{-2} (0.8 – 1.3 cm yr^{-1}) per spring-neap cycle than in the highly degraded site with a range of 51.78 – 144.48 g m^{-2} (0.5 – 0.7 cm yr^{-1}) per spring-neap tide cycle. The accretion rates (in cm yr^{-1}) were extrapolated by multiplying the accretion rates (g m^{-2} converted to g cm^{-2}) per 14-

day spring-neap cycle, with the number of spring-neap tidal cycles (approx. 25) in a year and dividing it by the dry bulk density. Furthermore, accretion rates showed a negative relationship with decreasing distance from the creek (Fig. 12) and the regression analysis showed that the increase in accretion rate is significant with decreasing distance from the creek ($p = 0.0325$).

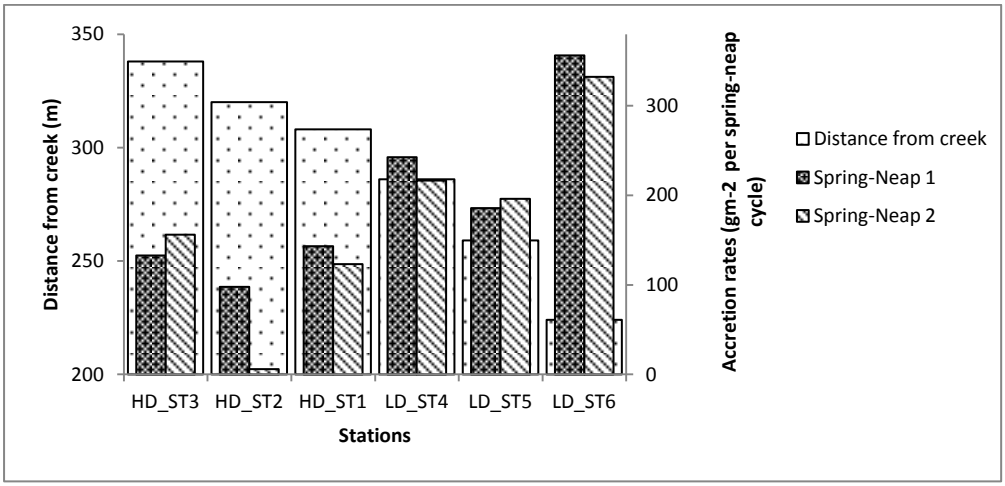

Figure 11: Showing sediment accretion rates in the different stations coupled with the relative proximity of stations to the creek. HD = highly degraded site and LD = less degraded site.

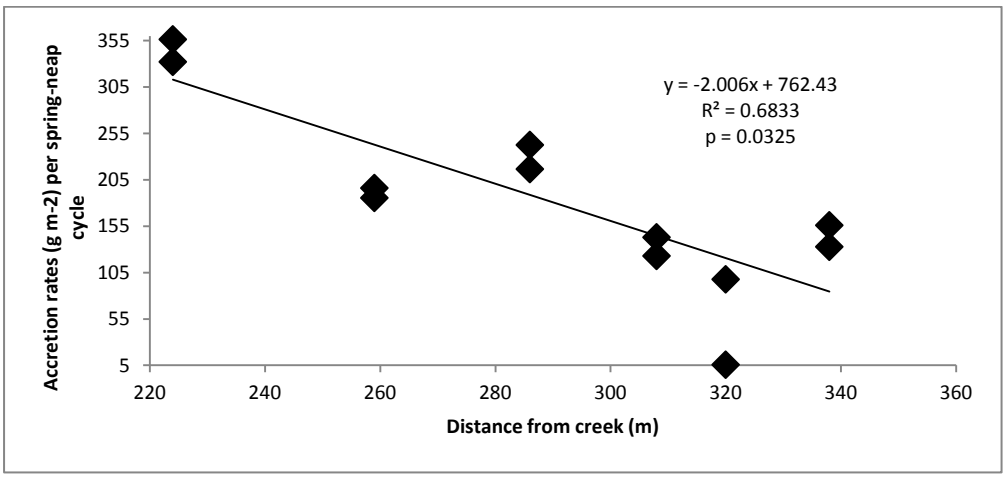

Figure 12: Showing the negative near-linear relationship between average accretion rates and the relative distance from the creek.

Accretion rates also showed a positive linear relationship with the amount of suspended sediment concentration (SSC) (Fig. 13). However, the regression analysis showed that the increase in accretion rate with with increasing SSC was not significant ($p = 0.099$).

An independent samples t-test was conducted to compare sediment accretion rates in less and highly degraded sites of Mwache Creek over two 14-day spring-neap cycles and there was a significant difference (df = 10, p = 0.00280) in sediment accretion rates between the two sites i.e. the sediment accretion rates were significantly higher in less degraded sites than in highly degraded sites. However, these t-test results are only based on 6 samples (2 spring-neap cycles for each of the 3 stations) per type of site and hence the results may not be regarded as conclusive. Furthermore, the effect of the vegetation and distance from the creek on sediment accretion is most probably not independent from the effect of other environmental conditions, such as the surface elevation of the station (this influences the tidal inundation frequency and height, and hence the supply of suspended sediments).

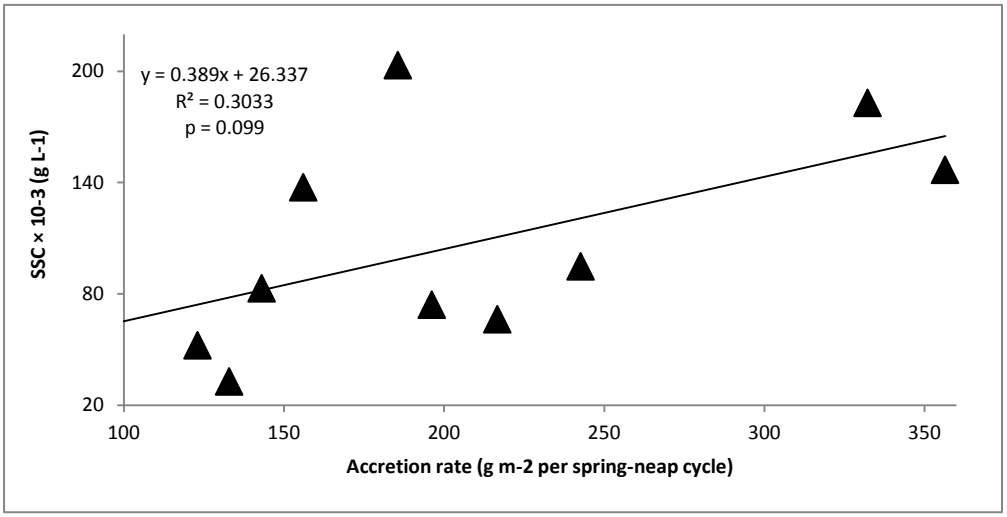

Figure 13: Showing the positive linear relationship between accretion rates and amount of suspended sediment concentrations (SSC). An increase in amount of SSC (sediment availability) translates to higher accretion rates.

3.4 Elevation change: Sedimentation-Erosion tables (SETs).

The mangrove surface elevation changes (in mm) derived from the SETs are summarized below (Fig. 14, 15) representing spatial and temporal variations. There was a discernible variation in elevation change (mm) both spatially and temporally in both sites (Fig. 14, 15). The y-axis represents the elevation change (in mm) over the twelve months taking April, 2012 (far left) as the reference value and measurements in the subsequent months measured relative to this reference value.

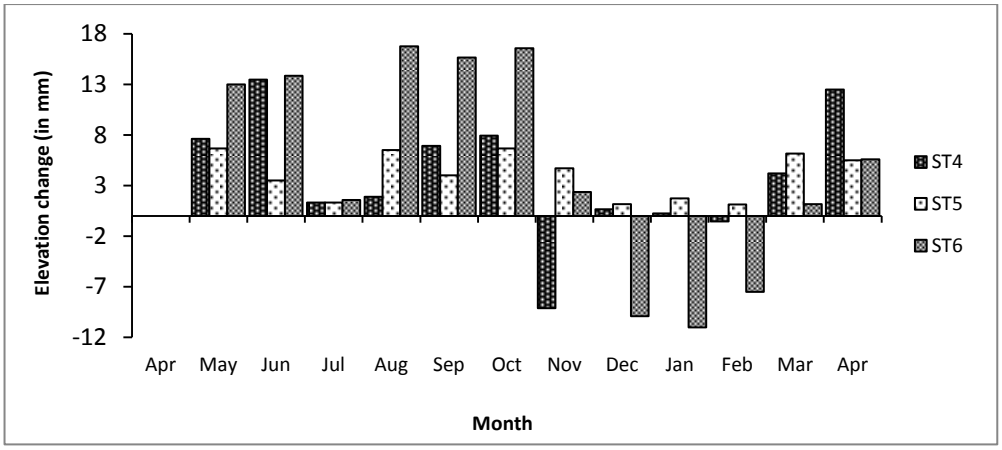

Figure 14: Mangrove surface elevation changes in less degraded sites derived from Sedimentation-Erosion tables over a year and showing shallow subsidence (negative values) and gained elevation (positive values). The y-axis represents the elevation change (mm) in different months between the periods April, 2012 – April, 2013 derived by taking the elevation value of April, 2012 as the reference value.

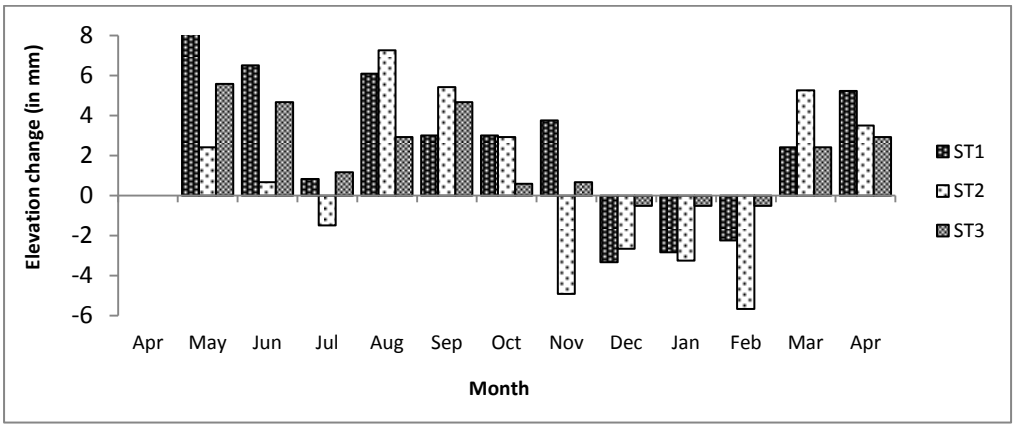

Figure 15: Mangrove surface elevation changes in highly degraded site derived from Sedimentation-Erosion tables over a year and showing shallow subsidence (negative values) and gained elevation (positive values). The y-axis represents the elevation change (in mm) in different months between the periods April, 2012 – April, 2013 derived by taking the elevation value of April,2012 as the reference value.

Despite the shallow subsidence observed of up to 11 mm per month, both sites showed annual elevation increase ranging between 2.92 – 5.22 mm yr^{-1} and 5.50 – 12.48 mm yr^{-1} in the highly degraded and less degraded site respectively. Statistical analyses (Table 1) showed that there were significantly higher rates of elevation change in the less degraded sites as compared to the highly degraded sites (t-test, df = 76, p = 0.0188) but there was no significant difference in elevation change within the sites (between stations) in highly degraded (one-way ANOVA, df = 2, p = 0.47) or less degraded sites (one-way ANOVA, df = 2, p = 0.95).

Table 1: Showing the results of unpaired t-test and one – way ANOVA statistical analyses performed on Sediment-Erosion tables (SETs) data, suspended sediment concentrations (SSC) and accretion rates. HD = highly degraded site, LD = less degraded site and S-N = Spring-Neap.

Data	Test	Site	P-value	DF	SS	MS	F-Ratio	Significance
SETs	Unpaired t-test	Between sites	0.0188	76			2.472	***
SETs	ANOVA	HD	0.4657	2	18.75	9.3732	0.7805	*
SETs	ANOVA	LD	0.9465	2	5.295	2.6477	0.05	*
Accretion	Unpaired t-test	Between sites	0.0028	10			1.7528	***
SSC	Unpaired t-test	Between S-N cycles	0.8097	8			1.3754	*

* = NOTsignificant *** = Significant

3.5 Water levels and sea level rise

The surface elevations of the stations were estimated at 3.52, 3.17 and 3.05 m L.A.T for stations 2, 4 and 5 respectively. These elevation estimates were obtained by matching the high water levels measured by the tide gauge station at Mombasa and the relative water depths that we measured at the mangrove stations with the divers. This was done by identifying the time at which maximum water depths (m) recorded by the divers matched with high water levels (m L.A.T) recorded by the tide gauge. By adding estimated elevation to the water depth, the elevation that caused the water depth and high water levels to match represented the estimated surface elevation (m L.A.T) at that particular point. Therefore, the sum of the estimated surface elevation and the water depth (measured by the diver) gave the estimated water level (m L.A.T) that matched in all stations at a particular inundation time (Fig. 16).

Based on the estimated elevations (m L.A.T) and inundation classes as described in Bosire *et al*. (2003), ST2 can be placed under inundation class 5 since it is only inundated by exceptional high tides. On the other hand ST4 and ST5 corresponds to inundation class 1 and 2 inundated by all high and medium high tide instances in the semi-diurnal tidal cycle. The high water levels measured by tide gauge (m L.A.T) and high water depth measured by divers showed a 50 minutes time lag between period of high water at the tide gauge and corresponding high water depth in the mangroves. This was taken into consideration when matching their peaks.

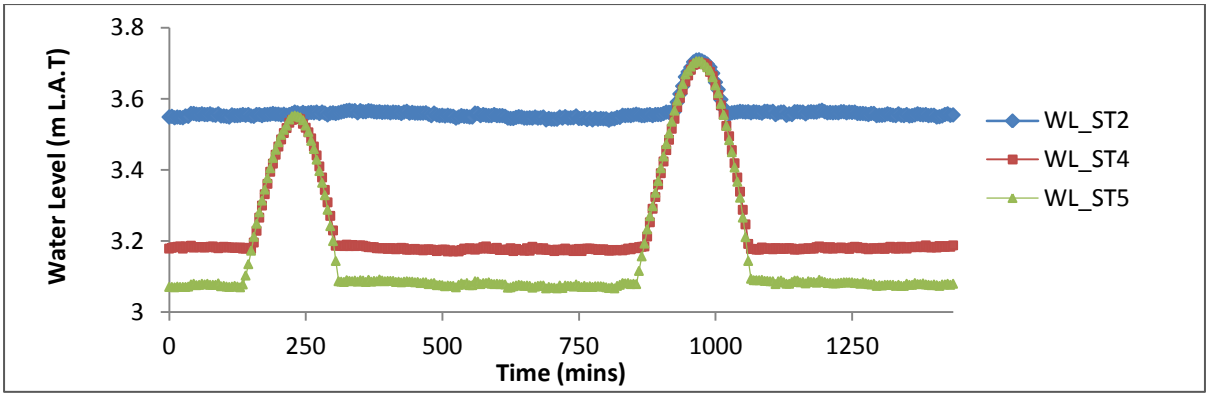

Figure 16: Showing the evolution of water levels (m L.A.T) in ST2, ST4 and ST5 with two peaks signifying moments of inundation in a semi-diurnal tide regime. Water level = Water depth by diver (m) + Estimated surface elevation (m L.A.T), Time is in minutes on August 19th, 2012 and WL=Water level (m L.A.T).

Mean sea level measurements (in m L.A.T) derived from Mombasa tide gauge data, showed an increase in mean sea level over the period 1986 – 2012 (Fig. 17). Infact, regression analysis showed that the increase in mean sea level over the period 1986 – 2012 is a significant ($p = 0.004513$). Based on the slope of the linear regression equation (Fig. 17), the longterm average rate of sea level rise in Mombasa is estimated at 3.1 mm yr^{-1} over the same period.

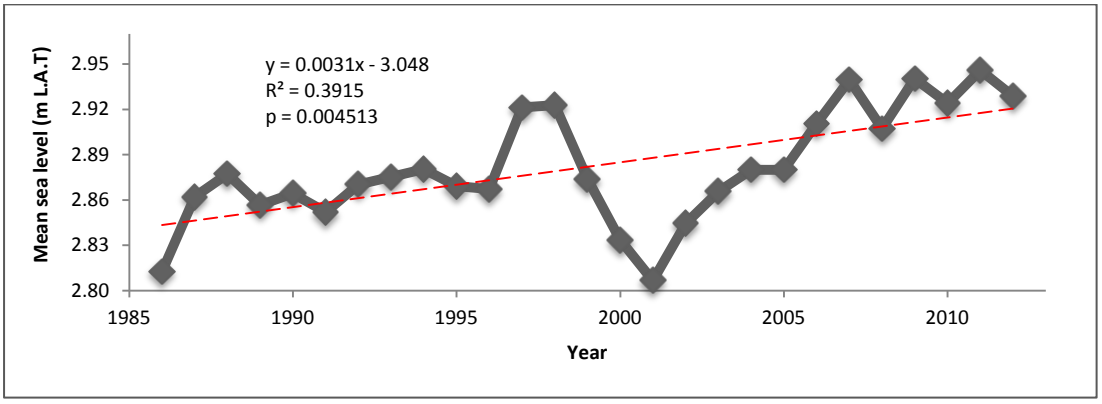

Figure 17: Showing an increasing trend of sea level in Mombasa over the years over the period 1986 – 2012.

3.6 Evaluation of model results

From the model simulations, the growth of mangrove surface elevation relative to the mean sea level showed a distinct variation when input variables were changed (Table 2). Different values for input variables were chosen based on the range of values that were measured in the field for these input variables. These input variables are; initial surface elevation of mangrove surface at the beginning of the simulation period (m L.A.T), incoming suspended sediment concentrations (kg m^{-3}), settling velocities of sediments in suspension

(m s^{-1}), dry bulk density of deposited sediment (kg m^{-3}), rates of organic sediment accretion (m yr^{-1}), and rates of sediment compaction (m yr^{-1}).

Table 2: Showing the model simulations by varying the various input variables and the final elevation attained by the mangrove surface. Different values for the input variables are based on the range of values measured in the field. Where dSorg/dt = rate of organic sediment accretion, dP/dt = compaction rates, SSC = Suspended sediment concentrations and E = Elevation

Simulation	Initial elevation, E (m L.A.T)	Dry bulk density (kg m^{-3})	Settling velocity (m s^{-1})	dSorg/dt (m yr^{-1})	dP/dt (m yr^{-1})	SSC (kg m^{-3})	Final elevation, E (m L.A.T)
1	2.95	590.00	0.002362	0.000481	-0.00282	0.102	4.3012
	3.05 [ST5]						4.3265
	3.17 [ST4]						4.3546
	3.25						**4.3734**
	3.40						4.4083
	3.52 [ST2]						4.4342
	3.75						4.4542
	4.25						4.6014
2	3.25	429.00	0.002362	0.000481	-0.00282	0.102	4.5281
		529.00					4.4292
		590.00					**4.3734**
		629.00					4.3406
		729.00					4.2600
3	3.25	590.00	0.0002871	0.000481	-0.00282	0.102	3.4269
			0.0005329				3.6087
			0.001086				3.9399
			0.002362				**4.3734**
			0.003011				4.4928
			0.004436				4.6544
4	3.25	590.00	0.002362	0.000281	-0.00282	0.102	4.3717
				0.000381			4.3726
				0.000481			**4.3734**
				0.000581			4.3742
				0.000681			4.3762
5	3.25	590.00	0.002362	0.000481	-0.00082	0.102	4.4009
					-0.00182		4.3871
					-0.00282		**4.3734**
					-0.00382		4.3603
					-0.00482		4.3471
6	3.25	590.00	0.002362	0.000481	-0.00282	0.076	4.2134
						0.086	4.2829
						0.096	4.3424
						0.102	**4.3734**
						0.128	4.4865

Model simulations showed that organic sediment accretion (dS_{org}/dt) causes a gradual predicted increase in sediment accretion rates and subsequent mangrove surface

elevation. Model simulations of current rates of dS_{org}/dt showed an almost identical simulated sediment accretion rates and predicted mangrove surface elevation (Fig. 18). Varying the amounts of suspended sediment concentrations (SSC) showed an influence to predicted sediment accretion rates and ultimately surface elevation (Fig. 19) with increased net mangrove surface elevation and predicted sediment accretion rates corresponding to high SSC values.

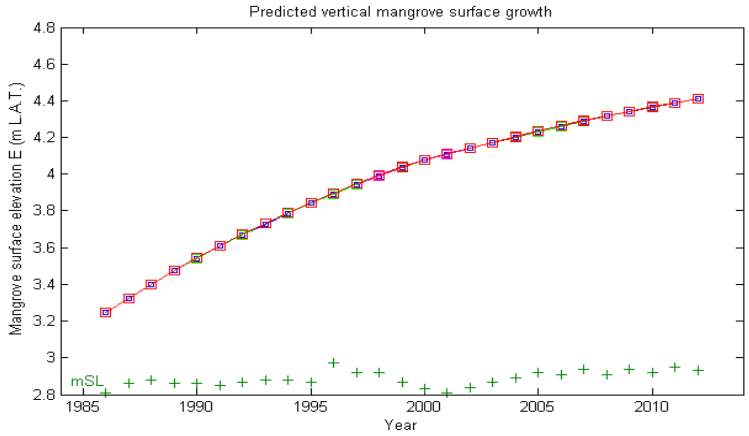

Figure 18: The almost identical effect of varying the rates of organic sediment accretion (*dSorg/dt*) on predicted vertical mangrove surface growth due to sediment accretion. Where mSL represents the mean sea level.

Simulating various settling velocities (W_s) showed that an increase in W_s resulted in an increased sediment accretion rate and predicted mangrove surface elevation over time however, very low settling velocities showed minimal effect on predicted sediment accretion rates and vertical mangrove surface elevation (Fig. 20).

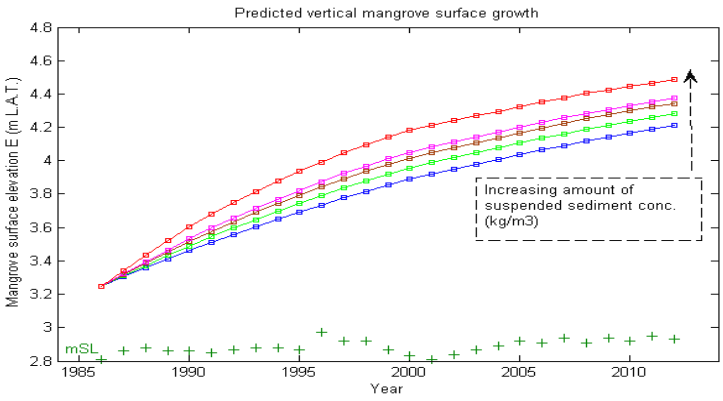

Figure 19: The effect on predicted vertical mangrove surface growth by varying the amount of suspended sediment concentration (kg m^{-3}). High amounts of sediments in suspension causes increased accretion translating to increased mangrove surface elevation.

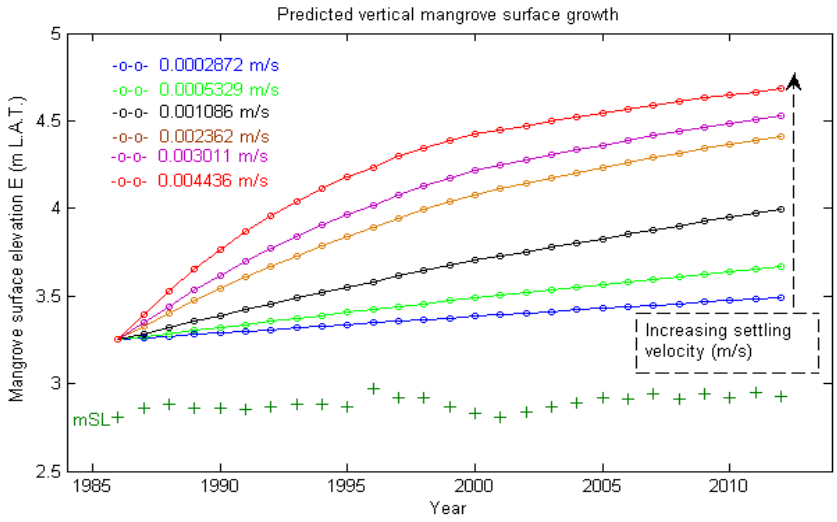

Figure 20: Showing the predicted mangrove surface growth by varying the settling velocity, low settling velocities have negligible effect on mangrove surface elevation with time.

Variations of the dry bulk density and compaction rates were also found to influence the mangrove surface elevation significantly (see Table 2). Less predicted elevation growth corresponded to high values of compaction rates and dry bulk density, however, the effect of varying compaction rates was very minimal (Fig. 21).

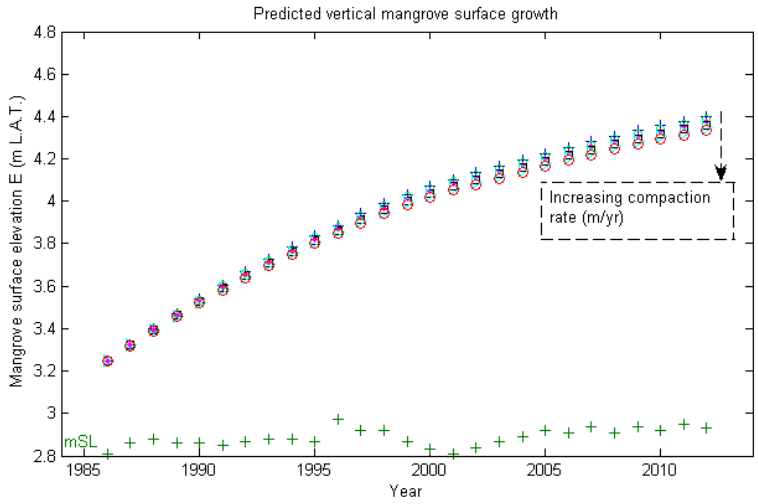

Figure 21: Showing the minimal and almost identical effect of varying the compaction rates on predicted mangrove surface growth and elevation.

Model simulations were done with elevation range of 2.95 – 4.25 m L.A.T (Table 2). With the current average sediment dynamics (accretion & compaction) and estimated elevation of our study site, model simulations showed a predicted gradual sediment accretion rates and subsequent mangrove surface growth (Fig. 22 and Table 2).

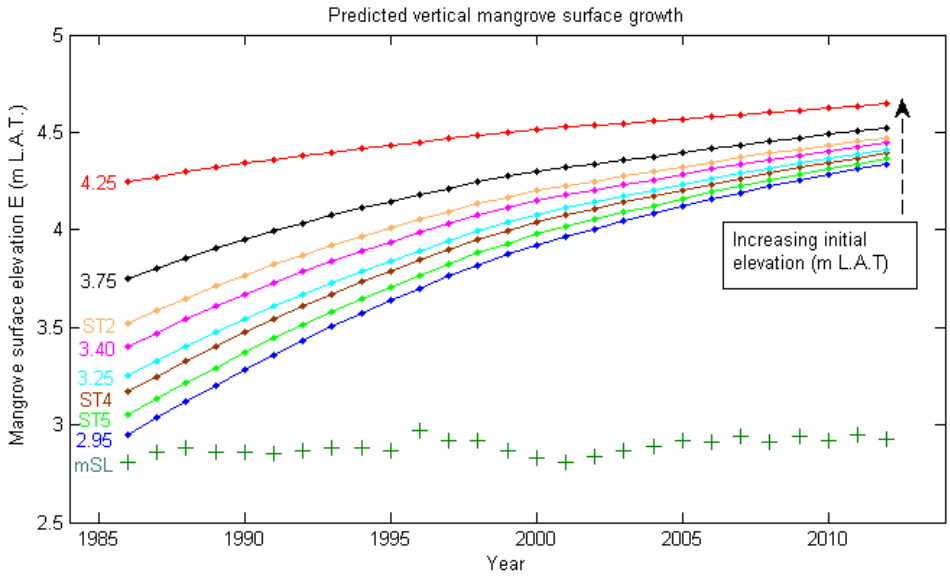

Figure 22: Showing the variation in predicted gradual mangrove surface growth and sediment accretion rates with different initial mangrove surface elevations, E (m L.A.T), where mSL = mean sea level.

However, the low elevation mangrove surfaces are characterized by an initial strong increase in elevation (Fig. 22) while the high initial elevation of mangrove surfaces showed minimal predicted sediment accretion rates and subsequent surface elevation (Table 2).

4. Discussion

Studies have shown that short-term temporal and spatial variations of sediment accretion in coastal forests are a function of availability of sediments, settling under gravity, proximity of site to the main creek channels, tidal variations and density of vegetation cover (Furukawa *et al*., 1997; McKee, 2011; Kumara *et al*., 2010; Saad *et al*., 1999; Temmerman *et al*., 2003a). Sediment accretion in our study varied spatially (between less and highly degraded site) with high values recorded in the less degraded site (Fig. 11). This could be explained by the fact that, dense vegetation in this site (stations ST4, ST5, ST6) causes increased wave attenuation and reduction of tidal currents, so that the resultant low velocities allowed fine sediments in suspension to be deposited. However, based on this study, the effect of vegetation cannot be separated from other environmental variables that may co-vary between the highly and less degraded sites. For example, the higher rates of sediment accretion and elevation change in the less degraded sites as compared to the highly degraded sites may also be attributed to the relative distances of the stations from the creek (Fig. 12) and their elevations with the farthest stations (ST1, ST2 & ST3) and those

with high elevations (ST2) experiencing less inundation and therefore less sediment accretion and elevation gain (Cahoon & Lynch, 1997; Saad *et al*., 1999). However, only 3 stations were studied in each site (less degraded and highly degraded) and the effect of vegetation is not independent from the effect of distance from the creeks and surface elevation of the mangrove. However these results provided an indicative trend conforming to earlier findings by other authors.

Our study, however, showed that sediment accretion rates decreased with increasing distances from the creek channel (Fig. 12) and this is attributed to gradual lowering of flow velocities and increasing friction of flow implying that sediments progressively settle out of suspension with increasing distance from a creek (Kumara *et al*., 2010; Saad *et al*., 1999; Temmerman *et al*., 2005b). Additionally, the negative relationship between accretion and distance from creek can also be explained as follows; the front mangroves (full high tide zone) are frequently exposed to tidal inundations and therefore experiences longer inundation periods than the back mangroves giving sediments in suspension more time to settle out. Also according to Saad *et al*. (1999) the front mangroves are comparatively lower relative to the sea level resulting in more inundation time. Together with their proximity to sediment source (the creek) this could explain the observed high sediment accretion rates in ST4, ST5 and ST6. Sediment accretion rates in this study also showed an increase with increasing amount suspended sediments concentrations (Fig. 13), meaning that increased sediments in suspension are a catalyst for increased accretion rate translating to mangrove surface elevation. But, according to Krauss *et al*. (2010) long-term predictions based on linear extrapolation could be a source of uncertainty due to annual and spatial variation of sea-level rise. However, year-long measurement and monitoring of sediment accretion rates is of essence to ascertain the seasonal effects on general sedimentation patterns. Because increased sediment input during rainy seasons could alter the sediment accretion rates. However, apart from the surface accretion rates measured in Mwache Creek, the specific contribution of vegetation canopy, below-ground root growth, and indeed the influence of above ground roots on the reduction of water flow and accretion of suspended sediments in the total net surface elevation change remains understudied in the mangroves of Kenya. This could lead to uncertainties, because species assemblage and associated root type, contribute locally in influencing the variability in sediment accretion (Furukawa *et al*., 1997; McKee *et al*., 2003). Surface erosion also

influences changes in elevation of a marsh/mangrove surface but in other sedimentation models, it is considered negligible and only tidal transport and sediment accretion are considered as the main factors affecting elevation changes (D'Alpaos, 2007a; French, 2006). In this study erosion was considered negligible but more studies are needed to ascertain what the effect of this within the whole system would be. The evolution of flow velocities with tidal flooding is also required to conclusively correlate the effect of attenuation of water flow velocities by mangroves to the sediment accretion rates variations.

There was an average annual increase in mangrove surface elevation (in mm) as measured by the SETs in both sites despite shallow subsidence during some months within the monitoring period. The less degraded site showed higher elevations as compared to the highly degraded site (Fig. 14, 15) and this could be explained by the different vegetation density between the sites with dense vegetation in the less degraded site. This would suggest then that dense vegetation would reduce flow velocities and allows sediments in suspension to settle out and the roots assisting in holding the sediments together to minimize resuspensions or erosion. The less degraded site also with its dense vegetation as compared to the highly degraded would experience higher surface elevations due to the additional effect of organic sediment accretion (an effect of litter production and belowground production) (Cahoon *et al*., 1995; McKee *et al*., 2007; Kumara *et al*., 2010). Highest elevations were observed between the months of April and November and this can be explained by increased terrestrial sediment input due to the long rains (April – August) and the short rains (October – November). Furthermore, the calculated elevation changes of 5 - 7 mm yr^{-1} and 8 - 13 mm yr^{-1} in the highly and less degraded sites respectively (extrapolated from 14-days accretion measurements by sediment traps) correlated well with elevation changes measured by SETs ranging between 2.92 – 5.22 mm yr^{-1} and 5.50 – 12.48 mm yr^{-1} in the highly and less degraded sites respectively.

The negative elevation changes (mm) recorded could be attributed to sediment auto-compaction due to overlying weight, decomposition of organic litter (Cahoon *et al*., 1995; McKee *et al*., 2007; Vandenbruwaene *et al*., 2011) and the effect of burrowing animals such as crabs (Dahdouh-Guebas *et al*., 2002; Micheli *et al*., 1991). The very low elevation changes between the months of December and March in both less and highly degraded site, is attributable to the fact that this period represent the driest months of the year and therefore loss of soil moisture could lead to shallow subsidence. These results

showed that modern rates of mangrove surface elevation could vary spatially, temporally and in magnitude within the same mangrove system supporting earlier research findings (McKee *et al*., 2007; Nyman *et al*., 2006). However, the survival of some marshes, mudflats and mangroves, despite high rates of subsidence, indicates that the combined effect of organic and inorganic accumulation processes can be adequate to sustain coastal ecosystems in the face of sea-level rise (McKee, 2011).

The water levels (m L.A.T) were same in the stations during inundation period and this is because mean high water levels as measured by the tide gauge corresponds to high water depths in the mangroves (Fig. 16). ST2 is not always inundated as compared to ST4 and ST5 and this could be attributed to its higher elevation and relative distance from the creek. Therefore, a threshold has to be achieved for inundation to occur at ST2. This result correlates well with the inundation classes of Kenyan mangroves as explained earlier and originally described in Bosire *et al*. (2003). The vegetation zonation as described in Dahdouh-Guebas *et al*. (2002) and Matthijs *et al*. (1999) also correlate well with this finding with ST2 being dominated by the high intertidal mangrove species specifically *A. marina* and *C. tagal* and ST4 and ST5 being characterized by full high tide zone mangrove species dominated by *R. mucronata* and *S. alba*. The 50 minutes lag of maximum water depth in the mangroves is attributed to the distance between the measuring tide gauge and the divers in the mangroves. The effect of this relatively large time lag between the tide gauge at Mombasa and the mangrove stations, could cause small differences in the level of high water level at Mombasa tide gauge and at the mangrove stations (due to deformation of the tidal wave during propagation through the creek and mangrove forest).

The relative sea level increase could be attributed to effects of global climate change including melting of glaciers and expansion of water due to increased temperatures. It is estimated that globally sea level raised by 1.8 mm yr^{-1} for the last century and sea level rise has recently accelerated up to 3 mm yr^{-1} (IPCC, 2007) which correlates well with the average rate of sea level rise in Mombasa for the period 1986-2012 which is estimated at 3.1 mm yr^{-1} (Fig. 17). This increased rise in sea level would affect most existing mudflats, marshes and mangrove ecosystems at different scales in different parts of the world. The sharp decline between the years 2000-2002, could be the effect of the 18.6 year lunar cycle (Euler effect) which causes either sharp fall or rise in sea level (Baart *et al*., 2012; French, 2006).

Model simulations confirmed that a variation in magnitude of environmental factors including organic sediment accretion (*dSorg/dt*), suspended sediment concentrations (*SSC*), settling velocities, compaction rates and initial mangrove surface elevation can combine to produce a cumulative effect that would eventually determine whether mangroves will keep up pace with rising sea level or not as reported in earlier research (Cahoon & Lynch, 1997; Day Jr. *et al*., 1999; McKee, 2011; Rybczyk *et al*., 2002; Temmerman *et al*., 2003a). Model simulations on dry bulk density (Table 2) showed an increasing variation with depth. This is attributable to compaction due to overlying weight and organic matter decomposition and model simulations showed that the current rates of compaction have minimal effect on the mangrove surface elevation (Fig. 21). Increased dry bulk density caused less mangrove surface growth suggesting that high values of dry bulk density causes higher compaction resulting in thinning of accreted sediment (refer to equation 2) hence reducing the mangrove surface elevation. Soil organic matter (SOM) amounts were highest in the less degraded site (Fig. 6) due to dense vegetation which is a source of organic litter. Accretion of organic matter from below-ground roots coupled with above-ground litter, determines the rate of dS_{org}/dt. The complex habitat specific production and decay processes makes dS_{org}/dt, difficult to be modeled easily (Temmerman *et al*., 2003b) and considering this and other authors (Allen, 1990; French, 2006), dS_{org}/dt is assumed to be constant which is acceptable in mineral-dominated environments (Temmerman *et al*., 2003b). Model simulation showed that the effect of varying the rates of organic sediment accretion (dS_{org}/dt) was minimal and almost identical conforming to the assumptions of the above authors (Fig. 18).

Model simulations showed the importance of suspended sediment (SSC) in helping the mangrove surface growth with higher SSC showing increased predicted sediment accretion rates and marsh elevation growth (Fig. 19, Table 2). This is because SSC is the primary source of sediments to the creek and therefore integral to mangroves keeping up with the rising sea level. However the rate of sea level rise moderates the rate at which mangroves/marshes need to accrete and avoid submergence (Temmerman *et al*., 2004) but the actual ability to maintain this equilibrium depends on availability of SSC. The amount of SSC in Mwache Creek might change considerably with seasons (Kitheka *et al*., 2003) with rainy season experiencing high sediment fluxes and long term monitoring is required to ascertain this effect.

The balance between mean sea level and surface elevation is the main process that determines the resilience of mangroves to effects of sea level rise. The model showed that increasing the initial mangrove surface elevation reduces the predicted sediment accretion rates and the rate of vertical growth of the mangrove surface (Fig. 22) and this is attributed to less inundation of the raised surface and therefore less sediment accretion (Vandenbruwaene *et al*., 2011). The initial gradual increase of mangrove surface elevation observed in our modeling, suggests that with inundation caused by tides, more sediment in suspension are brought into the mangrove forest and as they settle out of suspension, they cause vertical growth of mangrove surface due to the resultant accretion. However, the progressive decrease in mangrove surface elevation is caused by less inundation due to high mangrove surface elevation and signify the attainment of equilibrium between mangrove surface elevation and mean sea level and therefore no more elevation growth and subsequently the mangrove surface maintains it elevation relative to mean sea level (Allen, 1990; Temmerman *et al*., 2003a).

In terms of future research, it would be very interesting to do model simulations with different input values for the sea level rise rate, in order to determine the critical rates of sea level rise for which the mangrove surfaces are able or not able to keep up with sea level rise. It would be even more interesting to compare the results of this study with measurements from river-dominated estuaries and creeks along the Kenyan coast to see the magnitude of variation. In addition, there is a need to quantify model parameters in tropical ecosystems by more field and laboratory experiments. Therefore more research is needed for this to be achieved because several expressions used in the salt marsh models were derived for specific geographic regions.

5. Conclusion

The mangroves of Mwache Creek conform to the classical function of intertidal ecosystems of acting as sediment traps evident through the accretion rates and elevation changes observed. Although mangroves are known to lose their surface elevation relative to sea-level notwithstanding otherwise universal surface accretion (McKee *et al*., 2010) and with climate change likely to accelerate the relative sea-level rise (Gilman, 2008; Alongi, 2008), our mangroves are more likely to be more susceptible and threatened in the near future.

The average accretion rate of mangrove surfaces in Mwache Creek is estimated at 5 – 13 mm yr^{-1} which is higher than the average sea level rise in the 21st century of 1.8 mm yr^{-1} (IPCC, 2007) and higher than the average sea level rise of 3.1 mm yr^{-1} measured in Mombasa over the period 1986-2012, suggesting that mangroves of Mwache Creek are able to maintain or increase their elevation relative to the rising sea level. The higher average accretion rate in the mangroves closer to the creek channel is believed to be indicative for young prograding mangroves (Saad *et al*., 1999). Model simulations showed that organic sediment accretion is negligible to the cumulative net surface accretion and subsequent mangrove surface elevation and therefore suggesting that sediment accretion in Mwache Creek is mineral-dominated.

Current models in sediment transport dynamics are extremely simplified and are only a starting point for the representation of the complex interactions in intertidal ecosystems (Fagherazzi *et al*., 2012; French, 2006). The processes that affect sediment accretion and elevation changes in such environments are multi-faceted and complex and require more accommodating models that take into account most if not all the interactions.

Acknowledgement

This master thesis would not have been possible without the Flemish Inter–University Council (VLIR) masters scholarship. I am highly indebted to my promotor Prof. Dr. Stijn Temmerman and co-promotor Prof. Dr. Nico Koedam who guided and advised me throughout this study. I would also like to acknowledge the assistance and valuable input of Dr. Jared Bosire and Dr. Charles Magori both of Kenya Marine & Fisheries Research Institute (KMFRI).

The collection of field data was made possible through the assistance of colleagues and of particular mention are George Onduso, Angela Mbelase and Lillian Mwihaki. I also benefited immensely from valuable comments and technical assistance from several scientists from the Algemene Plantkunde en Natuurbeheer (APNA) research group at the Vrije Universiteit Brussels (VUB) and the Ecosystem management research group (ECOBE) at the University of Antwerp and of particular mention are Dr. Nabiul, Maris Tom, Alexandra Silinski, Marijke Ooms, Veerle Verschoren, Lennert Schepers, Anne Cools and Tom Van der Spiet. To all of you; *Ahsante sana*.

I am very grateful to my parents for their support and encouragement in my entire academic life. Senior ak Kabon, thank you for your selflessness and prayers to see us progress and I can only say "*Kongoi*". To ALL my course mates I can only say what an awesome two years. Special mention goes to Benson, Amina and my "big sister" Lizzy.

This work was supported by KMFRI's MASMA project on *'Resilience and adaptation of mangroves and dependent communities in the WIO region to the impacts of climate change'*, to which I am truly grateful.

References

Allen, J. R. L. (1990): Salt-marsh growth and stratification: A numerical model with special reference to the Severn Estuary, southwest Britain. *Marine Geology* **95(2)**: 77-96.

Allen, J. R. L. (1995): Salt-marsh growth and fluctuating sea level: Implications of a simulation model for Flandrian coastal stratigraphy and peat-based sea-level curves. *Sedimentary Geology* **100**: 21-45.

Allen, J. R. L. (1997): Simulation models of salt-marsh morphodynamics: some implications for high - intertidal sediment couplets related to sea-level change. *Sedimentary Geology* **113(3-4)**: 211-223.

Alongi, D.M. (2008): Mangrove forests: resilience, protection from tsunamis, and responses to global climate change. Estuarine, *Coastal and Shelf Science* **76(1)**: 1-13.

Baart, F., Pieter, H. G., de Ronde, J. and Koningsveld, J. (2012): The effect of the 18.6 year nodal cycle on regional sea level estimates. *Journal of Coastal research* **28(2)**: 511-516.

Bird, M. I., Fifield, L. K., Chua, S. and Goh, B. (2004): Calculating sediment compaction for radiocarbon dating of intertidal sediments. *Radiocarbon* **46(1)**:421–435.

Bosire, J. O., Dahdouh-Guebas, F., Kairo, J.G., Wartel, S., Kazungu, J. and Koedam, N. (2006): Success rates of recruited tree species and their contribution to the structural development of reforested mangrove stands. *Marine Ecology Progress Series* **325**: 85-91.

Bosire, J.O., Dahdouh-Guebas, F., Kairo, J.G. and Koedam, N. (2003): Colonisation of non-planted mangroves into reforested mangrove stands. *Aquatic Botany* **76:** 267 – 279.

Boumans, R. M. J., and J. W. Day, Jr. (1993): High precision measurements of sediment elevation in shallow coastal areas using Sedimentation - Erosion Table. *Estuaries* 16: 375 - 380

Cahoon, D. R., Lynch J. C., Perez, B. C., Segura, B., Holland, R. D., Stelly, C., Stephenson, G. and Hensel, P. (2002): High-Precision Measurements of Wetland Sediment Elevation: II. The Rod Surface Elevation Table. *Journal of Sedimentary Research* September ***72****:734-739*

Cahoon, D. R., & Lynch, J. C. (1997): Vertical accretion and shallow subsidence in a mangrove forest of south western Florida, USA. *Mangroves and Salt Marshes* **1**:173–186.

Cahoon, D. R., Reed, D. J., and Day, Jr. J. W. (1995): Estimating shallow subsidence in microtidal salt marshes of the southeastern United States: Kaye and Barghoorn revisited. *Marine Geology* **128**:1-9.

Cahoon, D.R., Hensel, P., Rybczyk, J. and Perez, B.C. (2002): Hurricane Mitch: impacts on mangrove sediment elevation dynamics and long-term mangrove sustainability. *USGS Open File Report* 03-184, 75 p.

Callaway, J.C. Borgnis, E. L., Turner, R. E., and Milan, C.S. (2012): Carbon sequestration and sediment accretion in San Francisco Bay tidal wetlands. *Estuaries and Coasts* **35**: 1163-1181

Chen, R. and Twilley, R. R. (1999): A simulation model of organic matter and nutrient accumulation in mangrove wetland soils. *Biogeochemistry* **44**: 93-118.

Christiansen, T., P. L. Wiberg, and T. G. Milligan (2000): Flow and sediment transport on a tidal salt marsh surface. *Estuarine Coastal and Shelf Science* **50:** 315-331.

Cochard, R., Ranamukhaarachchi, S. L., Shivakoti, G. P., Shipin, O. P., Edwards, P. J. and Seeland, K. T. (2008): The 2004 tsunami in Aceh and Southern Thailand: A review on coastal ecosystems, wave hazards and vulnerability. *Perspectives in plant ecology, evolution and systematics* **10(1)**: 3-40.

Dahdouh-Guebas, F., Verneirt, M., Cannicci, S., Kairo, J. G., Tack, J. F. and Koedam, N. K. (2002): An exploratory study on grapsid crab zonation in Kenyan mangroves. *Wetlands Ecology and Management* **10:** 179–187.

D'Alpaos, A., Lanzoni, S., Marani, M. and Rinaldo, A. (2007a): Landscape evolution in tidal embayments: Modeling the interplay of erosion sedimentation and vegetation dynamics. *J. Geophys. Res*., **112**, F01008, doi:10.1029/2006JF000537.

Day, Jr., J.W., Rybczyk, J., Scarton, F., Rismondo, A., Are, D. and Cecconi, G. (1999): Soil accretionary dynamics, sea-level rise and the survival of wetlands in venice lagoon: A field and modelling approach. *Estuarine, Coastal and Shelf Science* **49:** 607–628.

Diehl, T.H. (2008): A modified siphon sampler for shallow water: *U.S. Geological Survey Scientific Investigations Report* 2007–5282, 11 p.

Edwards, T.K. and Glysson, G.D. (1999): Field methods for measurement of fluvial sediment: U.S. Geological Survey Techniques of Water-Resources Investigations, book 3, chap.

C2, 80 p., accessed June 19, 2007, at http://pubs.usgs.gov/twri/twri3-c2/pdf/TWRI_3-C2.pdf.

Ellison, J.C. and Stoddart, R.D. 1991: Mangrove ecosystem collapse during predicted sea-level rise: Holocene analogues and implications. *Journal of Coastal Research* **7:** 151-165.

EPA (1983): Environmental monitoring and support laboratory, office of research and development. Methods for chemical analysis of water and wastes. Cincinnati, OH.

Fagherazzi, Sergio, *et al*. (2012): Numerical models of salt marsh evolution: Ecological, geomorphic, and climatic factors. *Reviews of Geophysics* **50(1)**.

Fagherazzi, S. and Priestas, A. M. (2010): Sediment and water fluxes in a muddy coastline: interplay between waves and tidal channel hydrodynamics. *Earth Surface Processes and Landforms* **35**: 284 -293

French, J. (2006): Tidal marsh sedimentation and resilience to environmental change: Exploratory modelling of tidal, sea-level and sediment supply forcing in predominantly allochthonous systems. *Marine Geology* **235(1-4)**: 119-136.

Furukawa, K. and Wolanski, E. (1996): Sedimentation in mangrove forests: *Mangroves and salt marshes* **1(1)**: 3-10.

Furukawa, K., Wolanski, E. and Mueller, H. (1997): Currents and sediment transport in Mangrove forests. *Estuarine, coastal and Shelf Science* **44**: 301 - 310.

Gilman, E. L., Ellison, J., Duke, N.C. and Field, C. (2008): Threats to mangroves from climate change and adaptation options: A review. *Aquatic Botany* **89**: 237-250.

IPCC (2007): Summary for Policymakers. In: Climate Change: The Physical Science Basis. Contribution of Working Group I to the Fourth Assessment Report of the Intergovernmental Panel on Climate Change [Solomon, S., D. Qin, M. Manning, Z. Chen, M. Marquis, K.B. Averyt, M.Tignor and H.L. Miller (eds.)]. Cambridge University Press, Cambridge, United Kingdom and New York, NY, USA.

Kairo, J.G., Kivyatu, B. and Koedam, N. (2002): Application of remote sensing and GIS in the management of mangrove forests within and adjacent to Kiunga marine protected area, Lamu, Kenya. *Environment, Development and Sustainability* **4**: 153-166

Kitheka, U. J., Ongwenyi, S. G. and Mavuti, M. K. (2002): Dynamics of suspended sediment exchange and transport in a degraded mangrove creek in Kenya. *Ambio* **31**: 580-587.

Kitheka, U. J., Ongwenyi, S. G. and Mavuti, K. M. (2003): Fluxes and exchange of suspended sediment in tidal inlets draining a degraded mangrove forest in Kenya. Estuarine, Coastal and Shelf Science 56: 655–667.

Kirui, B.K., Kairo, J.G. and Karachi, M. (2006): Allometric equations for estimating above ground biomass of Rhizophora Mucronata Lamk. (Rhizophoraceae) mangroves at Gazi Bay, Kenya. *Western Indian Ocean J. Mar. Sci*. **5(1)**:27-34.

Kirui, K.B., Kairo, J. G., Bosire, J., Viergever, K. M., Rudra, S., Huxham, M. and Briers, R. A. (2012): Mapping of mangrove forest land cover change along the Kenya coastline using Landsat imagery. *Ocean & Coastal Management* **xxx**: 1-6

Kirwan, M., and Temmerman, S. (2009): Coastal marsh response to historical and future sea-level acceleration. *Quaternary Science Reviews* **28**: 1801-1808.

Kumara, M. P., Jayatissa, L. P., Krauss, K.W., Phillips, D. H. and Huxman, M. (2010): High mangrove density enhances surface accretion, surface elevation change, and tree survival in coastal areas susceptible to sea-level rise. *Ecologia* **164**: 545-553.

Krauss, K. W., Cahoon, D. R., Allen, J. A., Ewel, K. C., Lynch, J. C., and Cormier, N. (2010): Surface elevation change and susceptibility of different mangrove zones to sea-level rise on Pacific High islands of Micronesia. *Ecosystems* **13**:129-143.

Leonard, L. A., and M. E. Luther (1995): Flow hydrodynamics in tidal marsh canopies. *Limnology and Oceanography* **40**: 1474-1484

Maris, T., Cox, T., Temmerman, S., De Vleeschauwer, P., Van Damme, S., De Mulder, T., Van den Bergh, E. and Meire, P. (2007): Tuning the tide: creating ecological conditions for tidal marsh development in a flood control area. *Hydrobiologia* **588**:31-43.

Matthijs, S., Tack, J., van Speybroeck, D. and Koedam, N. (1999): Mangrove species zonation and soil redox state, sulphide concentration and salinity in Gazi Bay (Kenya), a preliminary study. *Mangroves and Salt Marshes* **3:** 243–249.

McKee, K.L. & Faulkner, P.L. (2000a): Mangrove peat analysis and reconstruction of vegetation history at the Pelican Cays, Belize. *Atoll Research Bulletin* **468**: 46–58.

McKee, K. L., Cahoon, D. R., & Feller, I. C. (2007): Caribbean mangroves adjust to rising sea level through biotic controls on change in soil elevation. *Global Ecology and Biogeography **16*****(5)**: 545–556.

McKee, K. L. (2011): Biophysical controls on accretion and elevation change in Caribbean mangrove ecosystems. *Estuarine, Coastal and shelf science* **91(4)**: 475-483.

Micheli, F., Gherardi, F. and Vannini, M. (1991): Feeding and burrowing ecology of two East African mangrove crabs: *Marine Biology* **111**: 247-254.

Moeller, I., T. Spencer, and J. R. French (1996): Wind wave attenuation over saltmarsh surfaces: preliminary results from Norfolk, England,. *Journal of Coastal Research **12*:** 1009-1016.

Mohamed, M., Neukermans, G., Kairo, J.G., Dahdouh-Guebas, F. and Koedam, N. (2009): Mangrove forests in a peri-urban setting: the case of Mombasa (Kenya). *Wetlands Ecology and Management* **17**: 243-255.

Nyman, J. A., Walters, R. J., Delaune, R. D. and Patrick, Jr. W. H. (2006): Marsh vertical accretion via vegetative growth. *Estuarine, Coastal and Shelf Science* **69**: 370 - 380.

Rinaldo, A., Fagherazzi, S., Lanzoni, S., Marani, M. and Dietrich, W. E. (1999a): Tidal networks: 2. Watershed delineation and comparative network morphology. *Water Resources Research* **35(12)**: 3905–3917, doi:10.1029/1999WR900237.

Rybczyk, J. M. and Cahoon, D. R. (2002) : Estimating the potential for submergence for two wetlands in the mississippi river delta. *Estuaries* **25(5)**: 985–998.

Rybczyk, J. M., Callaway, J. C. and J. W. Day (1998): A relative elevation model for a subsiding coastal forested wetland receiving wastewater effluent. *Ecol. Modell.*, **112(1)**: 23‑44. doi:10.1016/S0304-3800(98)00125-2.

Saad, S., Husain, M. L., Yaacob, R. and Asano, T. (1999): Sediment accretion and variability of Sedimentological characteristics of a tropical estuarine mangrove: Kemaman, Terengganu, Malaysia. *Mangrove Marshes* **3**: 51 - 58.

Schmitz, N., Verheyden, A., Beeckman, H., Kairo, J.G. & Koedam, N. (2006): Influence of a salinity gradient on the vessel characters of the mangrove species Rhizophora mucronata. *Annals of botany* **98**: 1321-1330.

Spalding, M., Kainuma, M. and Collins, L. (2010): World Atlas of Mangroves. UNEP-WCMC. Cambridge.

Struyf, E., Temmerman, S. and Meire, P. (2005): Dynamics of biogenic Si in freshwater tidal marshes: Si regeneration and retention in marsh sediments (Scheldt estuary). *Biogeochemistry*. DOI 10.1007/s10533-006-9051-5.

Temmerman S., Govers, G., Meire, P. and Wartel, S. (2003a): Modelling long-term tidal marsh growth under changing tidal conditions and suspended sediment concentrations, Scheldt estuary, Belgium. *Marine Geology* **193**: 151-169.

Temmerman S, Govers G, Wartel S, Meire P (2003b): Spatial and temporal factors controlling short-term sedimentation in a salt and freshwater tidal marsh, Scheldt estuary, Belgium, SW Netherlands. *Earth Surf Process Landf* **28**:739–755.

Temmerman, S., Govers, G., Wartel, S. and Meire, P. (2004): Modelling estuarine variations in tidal marsh sedimentation: Response to changing sea level and suspended sediment concentrations. *Marine Geology* **212**: 1 – 19.

Temmerman, S., Bouma, T. J., Govers, G. and Lauwaet, D. (2005a): Flow paths of water and sediment in a tidal marsh: Relations with marsh developmental stage and tidal inundation height. *Estuaries* **28(3)**: 338–352.

Temmerman, S., Bouma, T. J., Govers, G., Wang, Z. B., De Vries, M. B. and Herman P. M. J. (2005b): Impact of vegetation on flow routing and sedimentation patterns: Three-dimensional modeling for a tidal marsh. *J. Geophys. Res.* **110**: F04019, doi:10.1029/2005JF000301.

Thomas, S. and Ridd. P. V. (2004): Review of methods to measure short time scale sediment accumulation. *Marine Geology* **207**: 95 – 114.

Tomlinson, P.B. (1986): The Botany of Mangroves. Cambridge University Press. *Cambridge tropical biology series*. 413 pp.

Vandenbruwaene, W., Maris, T., Cox, T.J.S., Cahoon, D.R., Meire, P. and Temmerman S. (2011): Sedimentation and response to sea-level rise of a restored marsh with reduced tidal exchange: Comparison with a natural tidal marsh. *Geomorphology* **130**: 115-126.

Wang, A. (2010): A simplified conception model for salt marsh sediment accretion rate calculation: Response to changing suspended sediment concentration-A case study of Wanggang salt marsh, Jiangsu Province, China. *Frontiers of Earth Science in China* **4**: 403-409.

Wentworth, C. K. (1922): A scale of grade and class terms for clastic sediments. *Journal of Geology* **30**: 377–392.

Woodroffe, C. (1992): Mangrove sediments and geomorphology, in Tropical Mangrove Ecosystems, *Coastal Estuarine Stud.*, vol. 41, edited by A. I. Robertson and D. M. Alongi, pp. 7–41, AGU, Washington, D. C., doi:10.1029/CE041p0007.

Woodroffe, C. (1985): Studies of a mangrove basin, Tuff crater New Zealand: III. The flux of organic and inorganic particulate organic matter. *Estuarine, Coastal and Shelf Science* **20**: 447-461.

Appendices

Appendix A

a) Highly degraded site with dead wood stumps b) Less degraded site

The highly degraded site (a) is due to massive human exploitation for fuel firewood and building material by local community and partly due to massive sedimentation during the 1997-1998 El Niño while site (b) represents the less degraded and more pristine mangrove forest with minimal human and natural impacts. Photos were taken on the 5th of September 2012 at Mwache Creek.

Appendix B

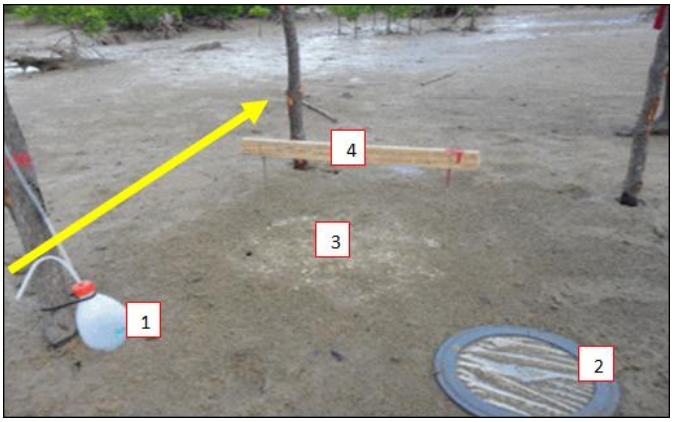

The field set up comprising of (1) Siphon sampler (2) Sediment trap (3) Feldspar marker and (4) Sedimentation-erosion table and the yellow arrow representing the direction of flood tide. Photo was taken on the 18th of August, 2012 at Mwache Creek during low tide.

Appendix C

a) Cera-diver

b) Baro-diver

Photos were taken on the 18th of August, 2012 at Mwache Creek during low tide. The Cera-diver tied to the mangrove root (a) as close as possible to the mangrove measures water and atmospheric pressure (when it is not submerged) while the Baro-diver tied to the mangrove stem (b) as high as possible to avoid contact with water measures only the atmospheric pressure. The difference between the water pressure measured by Cera-diver and the atmospheric pressure measured by the Baro-diver gives the hydrostatic pressure which can be transformed into an approximate water column above mangrove surface. The water column (WC) above the diver can be expressed as:

$$WC = 9806 * (p_{diver} - p_{baro}) / \rho . g$$

where p is the pressure in cmH_2O, g is the acceleration due to gravity (9.81 m s^{-2}) and ρ is the density of the water (1,000 kg m^{-3}). The water columns and subsequent water levels derived from the diver instruments are referenced to a fixed datum and in this study we referenced our water depths and water levels to the lowest astronomical tide (L.A.T).

Appendix D

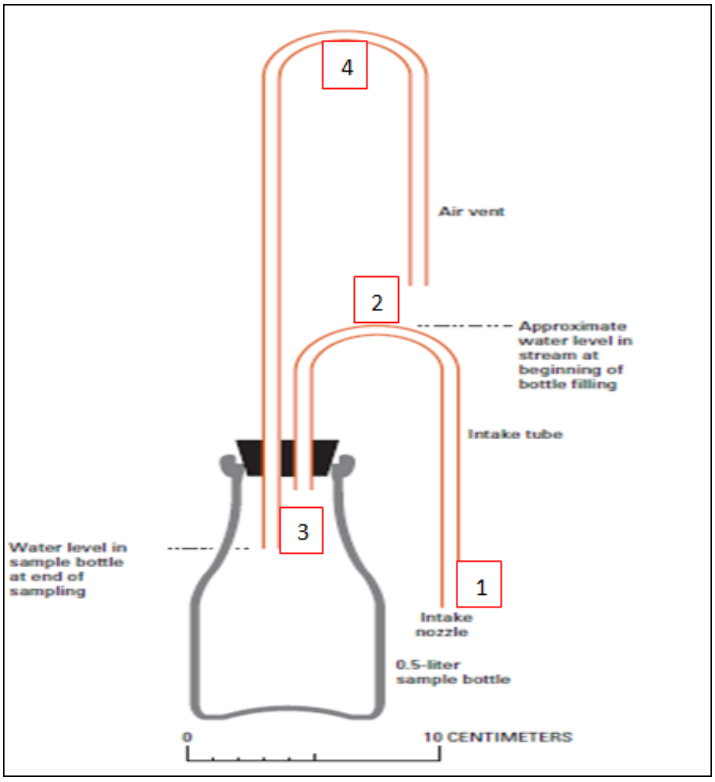

This is a modified siphon sampler with its components (Diehl, 2008). The operation of a siphon sampler is simple and as tide water flows into the mangrove forest and reaches the level of intake nozzle [1], water enters the tube and continues to move until it reaches level [2]. When water levels rise past level [2], a siphon is created and sample bottle start to fill. As the water level in the sample bottle reaches the bottom end of the exhaust port [3], filling is substantially completed; however, a small amount of additional water, equal to the water volume in the exhaust tube between levels [3] and [4], enters the bottle after the water level rises past level [3].